

# Differential leg and trunk operation during skipping without and with hurdles in bipedal Japanese macaque

Reinhard Blickhan<sup>1</sup>  | Emanuel Andrada<sup>2</sup>  | Eishi Hirasaki<sup>3</sup> | Naomichi Ogihara<sup>4,5</sup> 

<sup>1</sup>Science of Motion, Friedrich-Schiller-University, Jena, Germany

<sup>2</sup>Faculty of Social and Behavioural Sciences, Institute of Zoology and Evolutionary Research, Friedrich-Schiller-University, Jena, Germany

<sup>3</sup>Center for the Evolutionary Origins of Human Behavior, Kyoto University, Inuyama, Aichi, Japan

<sup>4</sup>Department of Mechanical Engineering, Keio University, Yokohama, Japan

<sup>5</sup>Department of Biological Science, Graduate School of Science, The University of Tokyo, Tokyo, Japan

## Correspondence

Reinhard Blickhan, Science of Motion,  
 Friedrich-Schiller-University, 07749 Jena,  
 Germany.

Email: [reinhard.blickhan@uni-jena.de](mailto:reinhard.blickhan@uni-jena.de)

## Funding information

DFG, Grant/Award Numbers: BL 236/28-1,  
 FI 410/16-1; Japan Society of Promotion of  
 Science; Primate Research Institute, Kyoto  
 University

## Abstract

When locomoting bipedally at higher speeds, macaques preferred unilateral skipping (galloping). The same skipping pattern was maintained while hurdling across two low obstacles at the distance of a stride within our experimental track. The present study investigated leg and trunk joint rotations and leg joint moments, with the aim of clarifying the differential leg and trunk operation during skipping in bipedal macaques. Especially at the hip, the range of joint rotation and extension at lift off was larger in the leading than in the trailing leg. The flexing knee absorbed energy and the extending ankle generated work during each step. The trunk showed only minor deviations from symmetry. Hurdling amplified the differences and notably resulted in a quasi-elastic use of the leading knee and in an asymmetric operation of the trunk.

## KEY WORDS

gait, joint angles, macaque locomotion

## 1 | INTRODUCTION

Macaques in traditional saru-mawashi shows are trained in bipedal posture and locomotion. This offers a vanishing chance to investigate the possibilities and limits of bipedal locomotion in nonhuman primates. The macaques were easily motivated by the caregivers to walk bipedally. However, despite spectacular jumps, the caregivers never observed bipedal running. In previous studies, we found that a variety of running gaits could be provoked (Ogihara et al., 2018). These entail symmetrical gaits (Hildebrand, 1977) such as aerial running and grounded running, a gait classified dynamically as a

running gait without aerial phases. However, the macaques also preferred skipping during fast locomotion. Skipping is a bipedal running gait characterized by deviations from symmetrical, out-of-phase operation of the two legs resulting in a double support and flight phase during one stride (Figure 1a; Minetti, 1998). The trailing leg absorbs the impact from the aerial phase. The leading leg touches the ground before the lift off of the trailing leg, generating a short double support period, and then pushes the skipper to the next aerial phase. In human skipping, two modes are distinguished: (i) bilateral skipping (high knee skips) and (ii) unilateral skipping (bipedal gallop). In bilateral skipping, the roles of the left and right legs switch with each

This is an open access article under the terms of the [Creative Commons Attribution-NonCommercial-NoDerivs](#) License, which permits use and distribution in any medium, provided the original work is properly cited, the use is non-commercial and no modifications or adaptations are made.

© 2024 The Authors. *Journal of Experimental Zoology Part A: Ecological and Integrative Physiology* published by Wiley Periodicals LLC.

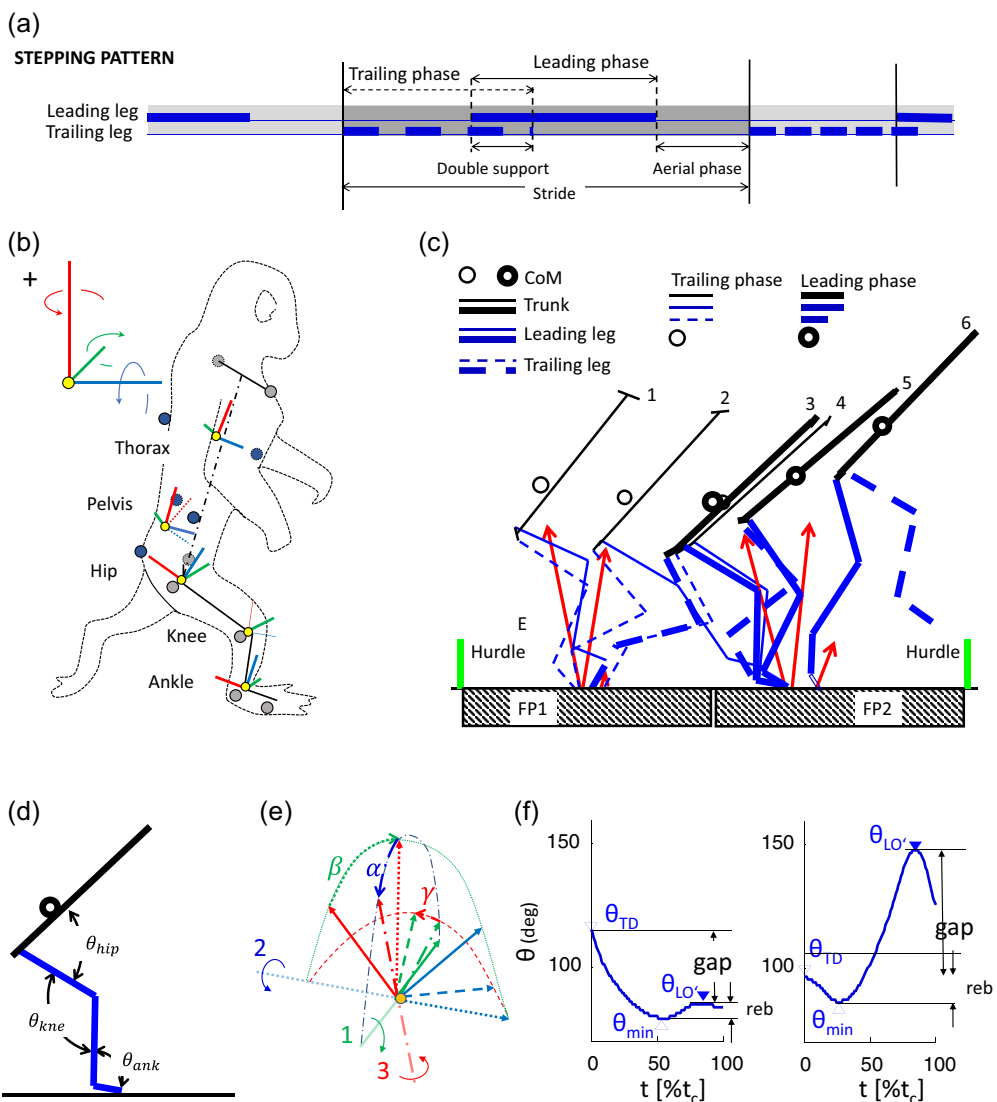


**FIGURE 1** Gait, markers, angles, coordinate system, and rebound. (a) The stepping pattern during unilateral skipping and unilateral skipping across hurdles entails both a double support period and an aerial phase, defining the leading and trailing leg. The gait cycle starts with the touch down (dashed vertical line) of the trailing leg, followed by the touch down of the leading leg with a double support until lift off (dashed vertical lines) of the trailing leg. The aerial period starts with the lift off of the leading leg. The stride ends with the touch down of the trailing leg after the flight phase. (b) Location of markers and coordinate systems. Marker location: left and right acromion; T10; sternum xiphoid; left and right anterior superior iliac spine (ASIS); sacrum; greater trochanter; lateral epicondyle; lateral malleolus; 5th metatarsal head. Markers on the contralateral leg not depicted. Black lines: HAT (dash-dotted), thigh, shank, foot (solid lines). Coordinate systems at thorax, pelvis, hip, knee, and ankle: yellow, origin; blue,  $\vec{e}_x$ ; green,  $\vec{e}_y$ ; red,  $\vec{e}_z$ . Pelvis: dashed, initial system using the markers; solid, system after touch down with  $\vec{e}_z$  parallel to HAT. Knee:  $\vec{e}_y$ , hinge joint assumed. (c) Stick-figures for a skipping stride across hurdles. 1: touch down trailing leg; 2: midstance trailing phase; 3: touch down leading leg; 4: lift off trailing leg; 5: midstance leading phase; 6: lift off leading leg. Red: Ground-reaction forces. Green: Hurdles. Hatched: force plates (FP1,2). (d) Enclosed joint angles at hip  $\theta_{\text{hip}}$ , knee  $\theta_{\text{kne}}$ , and ankle  $\theta_{\text{ank}}$ . (e) Rotation sequence: The distal system (solid arrows) is rotated to the proximal system (dashed arrows) by the first rotation (1),  $\beta$  (no prime, dotted) around  $\vec{e}_y$ , the second (2),  $\alpha$  ('', dash dotted) around the new  $\vec{e}'_x$ , and the third (3),  $\gamma$  ('', dashed) around the new  $\vec{e}''_z$ . (f) Rebound (reb) and rebound gap (gap) for examples of the macaque skipping across hurdles (knee left; ankle right).  $\theta_{\text{TD}}$ : maximum after touch down;  $\theta_{\text{min}}$ : local minimum;  $\theta_{\text{LO}}$ : local maximum before lift off.

stride. In the aerial phase, the leading leg is pulled forward and transformed into the trailing leg in the subsequent stride. In unilateral skipping, the legs maintain their alternating movement during each stride, and their roles remain consistent, that is, a left trailing leg will continue to be the left trailing leg in the next stride. We anticipated that the differential use of the leading and trailing legs, as identified

at the global level (Blickhan et al., 2023), could also be observed at the local level concerning joint kinematics and dynamics.

Skipping is common in birds (Alexander, 2004; Hayes & Alexander, 1983), and for many species, it merges into hopping (e.g., Verstappen et al., 2000). Humans learn bilateral skipping after walking and running at the age of about five with high pleasure

(Roncesvalles et al., 2001). During locomotion on the ground, sifakas selected skipping or hopping (Snyder & Schmitt, 2018; Wunderlich & Schaum, 2007). As in the wild, our macaques preferred quadrupedal transverse galloping both within and outside the shows (Kimura, 1992; Nakatsukasa et al., 2004, 2006). The shifted trot-gallop transition speeds for the front and hind limbs (Vilensky, 1983) point toward a weak coupling and may preadapt for the bipedal galloping preferred as bipedal gait in the high-speed range during our experiments.

The macaques employed a highly convenient method for skipping, characterized by short double supports, minor aerial phase, and minor vertical movement of the center of mass (CoM; Blickhan et al., 2023). Due to the adaptation to quadrupedal locomotion, hip extension is restricted (Ogihara et al., 2007) enforcing a rather compliant leg operation (Blickhan et al., 2018; Blickhan et al., 2023). Knowing that the macaques were capable of spectacular jumps, we questioned whether their upright posture, leg compliance, and stepping pattern at high speed limited their ability to engage in more dynamic skipping. To investigate this, we positioned small hurdles at the distance of a stride along our experimental track. This enforced seemingly effortless bipedal skipping marked by accentuated double support, elevated reaction forces, and notable differences in the global properties between the trailing and the leading legs (Blickhan et al., 2023; Ogihara et al., 2018).

During skipping, peak ground reaction forces and impulses did not differ between the leading and trailing legs (Blickhan et al., 2023). The impulse absorbed by the trailing leg equals the impulse generated by the leading leg to generate the aerial phase, with a crucial double support phase necessary for achieving sufficient speed during take-off. Also, stiffness of the leg telescope was not different. However, differences were noted at the global level regarding force components perpendicular to the leg axis (tangential forces) resulting in differences of the contribution of a damper assumed to be parallel to the leg spring and in a shift of the virtual pivot point (VPP). The latter indicates a point in the vicinity of the location of the CoM where the vectors of the ground-reaction forces cross (Maus et al., 2010; Vielemeyer et al., 2019). These differences, in conjunction with differences concerning leg rotation, are expected to lead to discrepancies in joint rotation and joint moments.

The similarity of peak ground-reaction forces and impulses has been documented for human skipping (Fiers et al., 2013). However, during bipedal grounded and aerial running, macaques utilize a more compliant leg compared to humans (Blickhan et al., 2018, 2023; Müller & Andrada, 2018; Pequera et al., 2021). The compliant legs along with their consequences were accentuated as being typical for nonhuman primates in general, and possibly advantageous also for our ancestors (Schmitt, 2003). In fact, we found that the vertical oscillations of the CoM were reduced as compared to human skippers (Blickhan et al., 2023). The enhanced leg compliance in the macaque may be largely due to a restricted hip joint extension (Ogihara et al., 2007) and to an adaptation to quadrupedal locomotion and may enforce a crouched leg posture (Blickhan et al., 2021). As compared to human skippers, the increased compliance of the legs should lead

to increased joint rotation. However, aerial running, compared to grounded running, was feasible with enhanced hip extension, but this extension was still far below human values (Blickhan et al., 2021). Hip extension could be increased in the leading phase and during hurdling, where higher aerial phases are necessary. Leg retraction was strongly supported by knee flexion, which in turn prevented human-like elastic rebound in the knee during aerial running. The quasi-elastic rebound at the leg level does not imply an elastic rebound at the joint level (Blickhan et al., 2021). The latter is crucial for human running economy. Does the differential use of the macaque leg foster a quasi-elastic rebound?

In symmetrical gaits such as walking, grounded running, and aerial running, the symmetrical operation of the legs is driven by a symmetrical operation of the trunk (Blickhan et al., 2021). Ignoring preferences, distractions, and changes in direction, trunk movement during a step with the right leg should mirror trunk movement during a step with the left leg. In human locomotion, with increasing speed, the movement of trunk segments decreases. This reduction may be partly due to the counter-movement of the arms (Prins et al., 2019) and partly due to trunk stiffening. Macaques, with a trunk mass of 61% body weight (Ogihara et al., 2009), exhibit limited arm movements and a “stiffening,” that is, reduced movement has been observed with higher running speed (Blickhan et al., 2021). Trunk pitch and leg rotation differ between the leading and trailing phases (Blickhan et al., 2023). The asymmetrical movement pattern of the legs predefined by the footfall pattern may also enforce a lateral bias and reduction of the mobility of the trunk segments.

The present study aims to clarify the differential leg and trunk operation during skipping in bipedal macaques by analyzing the rotations of the leg and trunk joints, and the leg joint moments.

## 2 | METHODS

### 2.1 | Subjects

The macaques were performed at the Suo Monkey Performance Association. The three adult male macaques (Ku| Po| Fu; age: 15|13|12 years; mass: 8.64|8.81|8.79 kg) had been trained for bipedal walking and performances since the age of about 1 year. The grand means (number of steps: 34|2|42) of leg lengths in the stance phases observed during grounded running and running was 0.399, 0.339, 0.405 m for the effective leg ( $l_0$ ) and 0.529, 0.465, 0.520 m for the virtual leg ( $l_{v0}$ ) respectively.

### 2.2 | Setup

The macaques were guided across a wooden track (length: 5 m) with two force plates embedded (0.4 m × 0.6 m). Skipping was induced with hurdles (height: 0.1 m) placed at the beginning and the end of the two force plates (0.81 m apart; Figure 1c). Kinematics and ground-reaction forces were captured with an eight-camera infrared motion capture

system (Oqus 3+, Qualisys) and the force plates (EPF-S-1.5KNSA13; Kyowa Dengyo), respectively, at a rate of 200 Hz.

## 2.3 | Procedure

The macaques were guided with a slack leash by an individual coach (caregiver). Reflective markers (Figure 1b; 14 mm diameter, Vicon) were attached to Velcro straps with double-sided tape. Macaques did not tolerate markers on their arms and head. A total of 15 markers were placed at the acromion (2), sternum xiphoid (1), tenth thoracic vertebra (1), anterior superior iliac spine (2), sacrum (1), greater trochanter (2), lateral epicondyle (2), lateral malleolus (2), and fifth metatarsal head (2). Joint centers of the knee, the ankle, and the metatarsals were calculated as half distance between medial markers placed in addition to the lateral markers during posing on the animal and during the trials by projecting from the lateral markers perpendicular to the main plane of movement of the knee. The location of the trochanter head was estimated by a similar projection from the greater trochanter-marker with a distance between the marker and trochanter head obtained from cadaver measurement (Ogihara et al., 2009).

## 2.4 | Ethical statement

The experiments were approved by the Animal Welfare and Animal Care Committee, Primate Research Institute, Kyoto University. All institutional guidelines were followed for this study. By rewards, the macaques were easily motivated to walk bipedally. They were used to jump across high hurdles. Speed was freely selected and experiments were stopped as soon as signs of unwillingness surfaced.

## 2.5 | Data evaluation

The joint centers of the knee, the ankle, and the metatarsals were calculated by projecting the half distance of the medial and lateral markers from the lateral markers perpendicular to the main plane of movement of the knee. The location of the hip was estimated as a projection perpendicular to the main plane of movement of the knee from the greater trochanter marker using a distance obtained from cadaver measurement (Ogihara et al., 2009). From this, the position of the segmental center of mass could be obtained using morphometric data (Ogihara et al., 2011). The center of mass of the trunk has been located on the line connecting mid hip joint (midpoint of the left and right joint centers) and mid shoulder. The CoP was registered by the force platform in combination with the markers at the lateral malleolus and fifth metatarsal head.

In compatibility with Blickhan et al. (2021), local co-ordinates were oriented as  $\vec{e}_z$ : vertical or along the long axis of segments,  $\vec{e}_y$ : medial, perpendicular to the plane defined by the adjacent segments, and  $\vec{e}_x = \vec{e}_y \times \vec{e}_z$  anterior (Figure 1b). For convenience and compatibility with literature, we described leg angles  $\theta_{\text{ankle}}, \theta_{\text{knee}}, \theta_{\text{hip}}$  enclosed by adjacent distal and proximal vectors ( $-\vec{e}_z^{\text{dist}}, \vec{e}_z^{\text{prox}}$ ) where the hip

angle was with respect to the HAT segment (Figure 1c,d). In addition, the Cardan angles ( $\beta, \alpha, \gamma$ ; rotation sequence  $y\ x\ z''$ ; Figure 1e) were calculated and termed extension or flexion, adduction or abduction, and lateral-medial rotation, respectively. At the hip,  $\beta$  was calculated with respect to the pelvis. Lumbar (lum) rotations between the pelvis and the thorax  $\beta$  were termed flexion ( $\beta$  decreasing) or extension ( $\beta$  increasing),  $\alpha$  lateral flexion, and  $\gamma$  torsion.  $\beta_{\text{lum}} = 0^\circ$  if the thorax and pelvis were aligned.  $\beta_{\text{lum}} < 0^\circ$  indicated the thorax was bent anteriorly with respect to the pelvis. For the movements of the pelvis and thorax with respect to the laboratory system of coordinates,  $\beta, \alpha$ , and  $\gamma$  were termed pitch (forward tilt), yaw (lateral lean), and roll (axial rotation), respectively.  $\beta_{\text{pel, tho}} = 0^\circ$  indicates alignment.  $\beta_{\text{pel, tho}} > 0^\circ$  indicated the anterior pitch of the segment. For relationships with respect to ISB definitions, see Blickhan et al. (2021).

Rebound of knee and ankle (Figure 1f) was calculated based on three quantities:  $\theta_{\text{TD}}$ : maximum after touch down within 10% of stride period, T;  $\theta_{\text{min}}$ : local minimum after touchdown;  $\theta_{\text{LO}}$ : maximum after minimum or value at lift off. Rebound, referring to range of values repeated during stance:  $\text{reb} = \min(\theta_{\text{TD}} - \theta_{\text{min}}, \theta_{\text{LO}} - \theta_{\text{min}})^\circ$ , rebound gap,  $\text{gap} = (\theta_{\text{LO}} - \theta_{\text{TD}})^\circ$ , relative rebound gap, with  $\text{rgap} = -1$  or  $+1$  for  $\text{reb} = 0$  and  $\text{rgap} = 0$  for  $\theta_{\text{LO}} = \theta_{\text{TD}}$ .

Planar (xz – plane) inverse dynamics was used to assess the proximo-distad joint torques (M), angular impulse ( $L_{\text{rot}} = \int_0^{t_c} M dt$ ), and rotational work ( $W_{\text{rot}} = \int_0^{t_c} M \cdot \dot{\beta} dt$ ) at the hip, knee ( $-\dot{\beta}$ ), and ankle joint, where  $t_c$  is contact time (contribution of segment inertia  $\leq 1.3\%$ ; moments of inertia scaled from Ogihara et al., 2011).

To facilitate statistics as well as the analysis of the motion of the trunk segments, only sequences where a full data set was available for both steps were selected for further analysis (Blickhan et al., 2023). This selection resulted in a sample of 18 (Ku:2; Fu : 8; Po : 8) strides for skipping and 31 (Ku:4; Fu : 22; Po : 5) strides for hurdling. Joint parameters and leg angles were investigated during stance. The description of trunk angles included the flight phase.

Froude speed was defined as  $Fr = v/\sqrt{gl_0}$ ,  $g$  gravitational acceleration.

The combined influence of leg (trailing vs. leading), Froude speed as a covariant, and the individuals was tested with a general linear model (hierarchic-type I with repetitions; Bonferroni correction  $f = 336$ , IBM®SPSS®). The repetition refers to the steps of the leading and the trailing leg within the same stride (Tables 1–3, Supporting Information: Tables S1–S3). This was complemented by univariate comparisons between skipping and hurdling considering the covariant Froude speed and the factor subject (Supporting Information: Tables S4–S6).

Custom software was written in MATLAB 14 (MathWorks).

## 3 | RESULTS

### 3.1 | Leg joint angles

During skipping the kinematics of the leading and trailing leg hardly differed from each other. During hurdling, a strong rebound was observed in the knee of the leading leg.

**TABLE 1** Comparison of leg joint angles including rebound properties of the leading and trailing leg as well as skipping and hurdling.

Var			Trailing Mean $\pm$ Std	Leading Mean $\pm$ Std	$p_{\text{tr-le}}$	$p_{\text{SK-HU,tr}}$
$\theta_{\text{hip}}$	TD (deg)	SK	101.5 $\pm$ 7.5	100.0 $\pm$ 7.2	n.s.	4.7E-03
		HU	95.8 $\pm$ 8.9	85.2 $\pm$ 11.3	6.6E-07	7.9E-13
	LO (deg)	SK	121.1 $\pm$ 7.4	128.6 $\pm$ 6.5	1.3E-03	2.6E-05
		HU	113.1 $\pm$ 13.1	123.5 $\pm$ 7.1	2.7E-11	6.2E-05
	rg (deg)	SK	27.7 $\pm$ 6.7	34.0 $\pm$ 2.9	7.4E-03	n.s.
		HU	24.3 $\pm$ 5.8	41.0 $\pm$ 5.5	3.8E-17	2.1E-06
	$\omega_{\text{max}}$	SK	255 $\pm$ 40	299 $\pm$ 60	n.s.	2.1E-02
		HU	218 $\pm$ 63	377 $\pm$ 60	1.4E-18	2.5E-10
$\theta_{\text{kne}}$	TD (deg)	SK	121.1 $\pm$ 7.7	121.7 $\pm$ 4.8	n.s.	4.1E-02
		HU	115.2 $\pm$ 5.8	121.0 $\pm$ 5.2	n.s.	1.7E+02
	LO (deg)	SK	83.4 $\pm$ 4.4	90.8 $\pm$ 7.5	1.0E-03	n.s.
		HU	83.8 $\pm$ 5.6	105.3 $\pm$ 4.9	8.6E-14	5.8E-16
	rg (deg)	SK	38.1 $\pm$ 6.1	31.6 $\pm$ 8.6	1.6E-04	n.s.
		HU	37.6 $\pm$ 5.6	21.2 $\pm$ 3.8	3.3E-13	6.8E-14
		SK	74 $\pm$ 52	98 $\pm$ 34	n.s.	3.4E-04
		HU	162 $\pm$ 78	229 $\pm$ 45	6.7E-04	3.8E-17
	reb (deg)	SK	2.60 $\pm$ 2.39	3.22 $\pm$ 1.76	n.s.	1.6E-02
		HU	7.18 $\pm$ 4.78	11.39 $\pm$ 2.85	1.5E-02	4.3E-16
	nreb ()	SK	0.10 $\pm$ 0.09	0.18 $\pm$ 0.09	n.s.	7.9E-02
		HU	0.20 $\pm$ 0.13	0.69 $\pm$ 0.16	1.1E-12	9.6E-17
$\theta_{\text{ank}}$	gap (deg)	SK	-22.72 $\pm$ 6.76	-15.43 $\pm$ 6.73	n.s.	2.4E-02
		HU	-29.42 $\pm$ 7.04	2.37 $\pm$ 5.75	3.9E-24	9.7E-21
	ngap ()	SK	-0.90 $\pm$ 0.09	-0.82 $\pm$ 0.09	n.s.	n.s.
		HU	-0.80 $\pm$ 0.13	0.14 $\pm$ 0.32	1.5E-23	1.1E-24
	TD (deg)	SK	98.5 $\pm$ 6.6	97.5 $\pm$ 10.7	n.s.	n.s.
		HU	96.4 $\pm$ 8.2	100.6 $\pm$ 5.3	n.s.	n.s.
	LO (deg)	SK	132.5 $\pm$ 9.1	139.4 $\pm$ 8.7	n.s.	n.s.
		HU	127.6 $\pm$ 12.8	138.9 $\pm$ 4.9	n.s.	n.s.
$\theta_{\text{ank}}$	rg (deg)	SK	62.4 $\pm$ 7.0	64.3 $\pm$ 13.8	n.s.	n.s.
		HU	66.0 $\pm$ 8.5	61.6 $\pm$ 6.8	n.s.	n.s.
		SK	849 $\pm$ 214	896 $\pm$ 250	n.s.	n.s.
		HU	822 $\pm$ 117	1124 $\pm$ 219	7.9E-13	4.6E-12
	reb (deg)	SK	11.38 $\pm$ 4.94	9.65 $\pm$ 4.17	n.s.	n.s.
		HU	11.65 $\pm$ 4.45	10.12 $\pm$ 3.14	n.s.	n.s.
	nreb ()	SK	0.18 $\pm$ 0.07	0.15 $\pm$ 0.06	n.s.	n.s.
		HU	0.18 $\pm$ 0.07	0.16 $\pm$ 0.04	n.s.	n.s.
$\theta_{\text{ank}}$	gap (deg)	SK	51.00 $\pm$ 6.30	54.66 $\pm$ 12.08	n.s.	n.s.
		HU	54.35 $\pm$ 7.94	51.48 $\pm$ 5.33	n.s.	n.s.
	ngap ()	SK	0.82 $\pm$ 0.07	0.85 $\pm$ 0.06	n.s.	n.s.
		HU	0.82 $\pm$ 0.07	0.84 $\pm$ 0.04	n.s.	n.s.

(Continues)

TABLE 1 (Continued)

Var			Trailing Mean $\pm$ Std	Leading Mean $\pm$ Std	$p_{tr-le}$	$p_{SK-HU,tr}$
$\alpha_{hip}$	TD (deg)	SK	-5.1 $\pm$ 4.0	-17.0 $\pm$ 9.4	5.3E-07	3.1E-10
		HU	-10.6 $\pm$ 5.4	-12.3 $\pm$ 7.7	n.s.	1.3E-04
	LO (deg)	SK	-15.2 $\pm$ 4.4	-19.1 $\pm$ 5.4	n.s.	9.1E-05
		HU	-10.2 $\pm$ 3.2	-14.2 $\pm$ 3.5	1.3E-03	1.7E-07
	rg (deg)	SK	12.3 $\pm$ 5.2	7.1 $\pm$ 2.8	n.s.	n.s.
		HU	11.6 $\pm$ 2.4	7.2 $\pm$ 1.8	8.0E-08	n.s.
		SK	70 $\pm$ 61	58 $\pm$ 41	n.s.	7.6E-13
		HU	179 $\pm$ 51	19 $\pm$ 62	1.2E-14	n.s.
$\beta_{hip}$	TD (deg)	SK	-84.6 $\pm$ 12.9	-82.3 $\pm$ 14.8	n.s.	1.7E-08
		HU	-100.4 $\pm$ 18.3	-106.5 $\pm$ 19.9	n.s.	9.8E-14
	LO (deg)	SK	-68.3 $\pm$ 12.7	-57.4 $\pm$ 15.2	2.0E-02	7.3E-13
		HU	-92.7 $\pm$ 21.9	-75.0 $\pm$ 20.5	5.6E-11	9.7E-11
	rg (deg)	SK	22.3 $\pm$ 7.9	29.4 $\pm$ 4.0	6.0E-03	1.8E-04
		HU	16.2 $\pm$ 4.7	32.3 $\pm$ 5.0	5.6E-20	n.s.
		SK	178 $\pm$ 57	258 $\pm$ 79	3.0E-03	n.s.
		HU	183 $\pm$ 50	294 $\pm$ 64	4.7E-15	8.7E-03
$\gamma_{hip}$	TD (deg)	SK	-4.9 $\pm$ 6.5	-8.7 $\pm$ 10.3	n.s.	2.8E-02
		HU	0.8 $\pm$ 4.5	-12.3 $\pm$ 4.6	5.9E-07	n.s.
	LO (deg)	SK	9.0 $\pm$ 8.5	-3.9 $\pm$ 8.0	1.1E-04	n.s.
		HU	11.7 $\pm$ 3.0	-7.9 $\pm$ 4.4	1.7E-18	1.3E-03
	rg (deg)	SK	19.2 $\pm$ 7.4	12.7 $\pm$ 4.4	3.2E-05	n.s.
		HU	16.3 $\pm$ 2.5	9.2 $\pm$ 2.4	4.0E-09	4.7E-03
		SK	270 $\pm$ 110	235 $\pm$ 65	n.s.	n.s.
		HU	246 $\pm$ 38	141 $\pm$ 60	3.3E-11	1.2E-09
$\alpha_{ank}$	TD (deg)	SK	22.0 $\pm$ 16.8	3.5 $\pm$ 5.1	n.s.	4.1E-10
		HU	6.8 $\pm$ 6.8	5.4 $\pm$ 5.2	n.s.	n.s.
	LO (deg)	SK	10.9 $\pm$ 7.8	15.6 $\pm$ 4.2	n.s.	4.9E-06
		HU	16.8 $\pm$ 3.1	18.4 $\pm$ 5.5	n.s.	3.0E-02
	rg (deg)	SK	25.8 $\pm$ 16.1	16.9 $\pm$ 3.5	4.2E-02	1.4E-04
		HU	16.7 $\pm$ 4.1	15.0 $\pm$ 4.7	n.s.	n.s.
		SK	202 $\pm$ 71	293 $\pm$ 101	n.s.	n.s.
		HU	270 $\pm$ 73	248 $\pm$ 136	n.s.	n.s.
$\beta_{ank}$	TD (deg)	SK	-80.4 $\pm$ 7.3	-82.5 $\pm$ 10.9	n.s.	n.s.
		HU	-83.6 $\pm$ 8.3	-79.3 $\pm$ 5.3	n.s.	n.s.
	LO (deg)	SK	-44.8 $\pm$ 11.6	-35.7 $\pm$ 12.1	n.s.	n.s.
		HU	-48.9 $\pm$ 15.8	-35.6 $\pm$ 6.2	n.s.	n.s.
	rg (deg)	SK	76.6 $\pm$ 20.7	72.4 $\pm$ 14.6	n.s.	n.s.
		HU	72.9 $\pm$ 9.2	68.1 $\pm$ 9.2	5.8E+00	n.s.

TABLE 1 (Continued)

Var		Trailing Mean $\pm$ Std	Leading Mean $\pm$ Std	$p_{tr-le}$	$p_{SK-HU,tr}$
$\gamma_{ank}$	TD (deg)	SK      935 $\pm$ 203	1005 $\pm$ 267	n.s.	n.s.
		HU      936 $\pm$ 128	1219 $\pm$ 251	1.2E-09	2.5E-09
	LO (deg)	SK      2.0 $\pm$ 3.4	-1.1 $\pm$ 1.1	n.s.	3.7E-03
		HU      -0.7 $\pm$ 0.9	-0.7 $\pm$ 1.4	n.s.	4.3E+01
	rg (deg)	SK      6.6 $\pm$ 8.7	14.0 $\pm$ 9.4	n.s.	n.s.
		HU      10.2 $\pm$ 7.6	15.6 $\pm$ 8.1	n.s.	n.s.
	rg (deg)	SK      25.1 $\pm$ 14.0	25.4 $\pm$ 5.0	n.s.	n.s.
		HU      22.5 $\pm$ 5.9	22.1 $\pm$ 7.1	n.s.	n.s.
		SK      395 $\pm$ 119	502 $\pm$ 112	n.s.	n.s.
	HU      441 $\pm$ 131	617 $\pm$ 203	3.4E-04	n.s.	

Note:  $\theta$ , enclosed joint angles;  $\alpha, \beta, \gamma$ , cardan angles adduction, extension, lateral-medial rotation; hip, knee, ank, leg joints; TD, touch down; LO, lift off; rg, range;  $\omega$ , angular velocity; reb, rebound; nreb, relative rebound; gap, gap; ngap, relative gap; SK, skipping; HU, hurdling;  $p_{tr-le}$ , comparison between trailing leading leg;  $p_{SK-HU,tr,le}$ , comparison between skipping and hurdling for the trailing (row SK) and the leading leg (row HU), respectively. Comparisons based on GLM with repetitions (Supporting Information: Table S1) and univariate GLM (Supporting Information: Table S4) Bonferroni  $f = 336$ ; n.s.,  $p > 0.05$ .

Hip enclosed angle,  $\theta_{hip}$ , and extension,  $\beta_{hip}$  (Figures 2a,b and 3a, Supporting Information: Figure S1a,b,d,e): The thigh was retracted until about 80%  $t_c$ . During hurdling, the hip of the leading leg was strongly extended from ca. 80 deg at touch down to 120 deg at lift off. In contrast, the movement range was reduced in the trailing leg as compared to the leading leg ( $\theta, \beta_{hip-rg}$ ; Figure 3a; Table 1). Maximum extension velocity ( $\omega_{\theta,\beta,hip-max}$ ) was higher in the leading than in the trailing leg (Table 1). The more experienced macaque (Ku) used a more extended hip in the trailing leg (Supporting Information: Figure S1a,d).

Hip adduction,  $\alpha_{hip}$  (Figures 2b and 3d, Supporting Information: Figure S1b): Hip abduction tended to increase during stance. During skipping,  $\alpha_{hip}$  at touch down was lower in the leading than in the trailing leg ( $\alpha_{hip-TD}$ ; Table 1). While hurdling, the range of  $\alpha_{hip}$  and the value at lift off in the trailing leg was higher than in the leading leg ( $\alpha_{hip-rg,LO}$ ; Table 1). Maximum abduction and adduction velocities were higher in the trailing than in the leading leg ( $\omega_{\alpha,hip-max}$ ; Table 1). Po used more adducted postures in the trailing leg and more abducted postures in the leading leg. Fu generated different time courses in the leading and trailing leg, with a minimum in the trailing leg, despite using different (left, right) legs as trailing legs.

Hip medial rotation,  $\gamma_{hip}$  (Figures 2b and 3e, Supporting Information: Figure S1b,e): The thigh rotated medially (ca. 12 deg) for the trailing leg, whereas for the leading leg, a lateral rotation was followed by a medial rotation. During skipping, this tendency could only be substantiated at lift off ( $\gamma_{hip-LO}$ ; Table 1). During hurdling, the hip operates in a medially oriented posture in the trailing leg and laterally in the leading leg ( $\gamma_{hip-TD,LO}$ ; Table 1). The range of rotations during stance is slightly higher in the trailing leg ( $\gamma_{hip-rg}$ ; Figure 3e; Table 1). Rotational velocity was reduced in the leading leg during hurdling ( $\omega_{\gamma,hip-max}$ ; Table 1).

Enclosed knee angle,  $\theta_{knee}$  (Figures 2a and 3, Supporting Information: Figure S1a,d): The range of knee movement was lower in the leading leg during both skipping and hurdling (Table 1). At lift off, the knee angle in the leading leg was higher in the leading than in the trailing leg both in skipping and hurdling ( $\theta_{knee-LO}$ ; Table 1). During skipping, the retractive flexion including a minor rebound was more pronounced in the trailing leg. The rebound reached quasi-elastic values during hurdling in the leading leg ( $\theta_{knee-reb,nreb,gap,ngap}$ ; Figures 2a and 3, Supporting Information: Figure S1a,d; Table 1).

$\theta, \beta_{ank}, \alpha_{ank}, \gamma_{ank}$  (Figures 2 and 3, Supporting Information: Figure S1): The ankle joint showed a strong extension (plantar flexion, ca. 80 deg) after about 20%  $t_c$  during skipping. This was slightly reduced while hurdling ( $\theta_{ank-rg}$ ). The maximum extension velocities for the leading leg exceeded the values of the trailing leg ( $\omega_{\beta,ank-max}$ ; Table 1). Macaque Po frequently landed in the trailing leg with fisted toes resulting in an unstable ankle flipping from strong flexion to dramatic extension within the first 30%  $t_c$  and a strongly adducted foot ( $\alpha_{ank}$ , Figure 3f, Supporting Information: Figure S1c,f) at touch down. During push off after 70%  $t_c$ , the ankle rotated medially ( $\gamma_{ank}$ , Figure 1c, Supporting Information: Figure S1c,f). Only minor quasi-elastic rebound was observed at the ankle ( $\theta_{ank-reb,nreb,gap,ngap}$ ; Table 1).

### 3.2 | Joint torques, rotational impulses, and work

The knee absorbed energy in both legs during skipping but only the trailing leg during hurdling.

During skipping, the moments,  $M$ , with respect to the hip, meandered around zero (Figure 4a, Supporting Information: Figure S2). This resulted in low rotational impulse,  $L$ , which for

**TABLE 2** Comparison of leg joint moments between the leading and trailing leg as well as skipping and hurdling.

			Trailing Mean $\pm$ Std	Leading Mean $\pm$ Std	$p_{tr-le}$	$p_{SK-HU,tr}$
						$p_{SK-HU,le}$
hip	$M_{min} [mg\ l_0]$	SK	-0.149 $\pm$ 0.046	-0.134 $\pm$ 0.030	n.s.	1.2E-02
		HU	-0.103 $\pm$ 0.043	-0.053 $\pm$ 0.038	3.5E-05	4.5E-09
	$M_{max} [mg\ l_0]$	SK	0.162 $\pm$ 0.106	0.170 $\pm$ 0.069	n.s.	6.5E-06
		HU	0.259 $\pm$ 0.062	0.342 $\pm$ 0.118	1.1E-04	2.1E-11
	$M_{rg} [mg\ l_0]$	SK	0.311 $\pm$ 0.085	0.304 $\pm$ 0.072	n.s.	n.s.
		HU	0.362 $\pm$ 0.050	0.396 $\pm$ 0.097	n.s.	6.7E-04
	$L_{rot} [mg\ l_0\ \sqrt{l_0/g}]$	SK	-0.020 $\pm$ 0.054	0.001 $\pm$ 0.031	n.s.	1.3E-03
		HU	0.028 $\pm$ 0.051	0.208 $\pm$ 0.094	8.5E-20	1.0E-19
kne	$M_{min} [mg\ l_0]$	SK	0.011 $\pm$ 0.023	0.019 $\pm$ 0.019	n.s.	n.s.
		HU	0.014 $\pm$ 0.021	0.181 $\pm$ 0.077	2.9E-22	8.3E-21
	$M_{max} [mg\ l_0]$	SK	-0.335 $\pm$ 0.061	-0.327 $\pm$ 0.061	n.s.	5.4E-06
		HU	-0.428 $\pm$ 0.059	-0.239 $\pm$ 0.040	5.4E-14	5.8E-08
	$M_{rg} [mg\ l_0]$	SK	0.000 $\pm$ 0.002	0.004 $\pm$ 0.005	n.s.	n.s.
		HU	0.001 $\pm$ 0.002	0.012 $\pm$ 0.008	2.7E-06	n.s.
	$L_{rot} [mg\ l_0\ \sqrt{l_0/g}]$	SK	0.335 $\pm$ 0.061	0.331 $\pm$ 0.063	n.s.	3.2E-06
		HU	0.430 $\pm$ 0.058	0.251 $\pm$ 0.039	4.0E-14	1.3E-07
ank	$M_{min} [mg\ l_0]$	SK	-0.252 $\pm$ 0.032	-0.238 $\pm$ 0.026	n.s.	1.1E-08
		HU	-0.321 $\pm$ 0.031	-0.146 $\pm$ 0.031	3.1E-18	1.5E-15
	$M_{max} [mg\ l_0]$	SK	-0.108 $\pm$ 0.027	-0.077 $\pm$ 0.029	1.8E-02	n.s.
		HU	-0.129 $\pm$ 0.037	0.013 $\pm$ 0.018	6.7E-19	3.1E-22
	$M_{rg} [mg\ l_0]$	SK	-0.037 $\pm$ 0.014	-0.023 $\pm$ 0.010	2.9E-04	n.s.
		HU	-0.033 $\pm$ 0.007	-0.002 $\pm$ 0.004	2.4E-17	2.8E-13
	$L_{rot} [mg\ l_0\ \sqrt{l_0/g}]$	SK	0.154 $\pm$ 0.041	0.126 $\pm$ 0.037	n.s.	6.6E-07
		HU	0.220 $\pm$ 0.040	0.196 $\pm$ 0.028	n.s.	3.0E-08
ank	$L_{rot} [mg\ l_0\ \sqrt{l_0/g}]$	SK	0.191 $\pm$ 0.045	0.150 $\pm$ 0.034	n.s.	1.2E-05
		HU	0.253 $\pm$ 0.041	0.199 $\pm$ 0.029	1.0E-06	9.3E-05
	$W_{rot} [mg\ l_0]$	SK	0.061 $\pm$ 0.032	0.059 $\pm$ 0.029	n.s.	2.3E-09
		HU	0.108 $\pm$ 0.034	0.115 $\pm$ 0.019	n.s.	1.1E-10
	$W_{rot} [mg\ l_0]$	SK	0.057 $\pm$ 0.022	0.071 $\pm$ 0.044	n.s.	n.s.
		HU	0.048 $\pm$ 0.018	0.134 $\pm$ 0.027	4.9E-14	3.3E-10

Note: hip, kne, ank, leg joints;  $M_{min,max,rg}$ , minimum, maximum, and range of joint moment (torque);  $L_{rot}$ , rotational impulse;  $W_{rot}$ , rotational work; SK, skipping; HU, hurdling;  $p_{tr-le}$ , comparison between trailing leading leg;  $p_{SK-HU,tr,le}$ , comparison between skipping and hurdling for the trailing (row SK) and the leading (row HU) leg. Comparisons based on GLM with repetitions (Supporting Information: Table S2) and univariate GLM (Supporting Information: Table S5) Bonferroni  $f = 336$ ; n.s.,  $p > 0.05$ .

hurdling differed between the leading and trailing leg (Table 2). Net rotational work extended the hip in both legs. The highest moments were generated at the knee. The rotational impulses did not differ between the two legs (Table 2). The high moments resulted in a high amount of work done at the knee while it was flexing. The ankle moments reached intermediate values (Figure 4a, Supporting

Information: Figure S2; Table 2), as did the rotational impulses. During hurdling, the impulses at hip and ankle were higher than during skipping. As compared to skipping, the work done in all joints of the leading leg was enhanced (Table 2). During hurdling, the work for ankle extension done in the leading leg exceeded the work at the trailing leg and the knee reached positive values (Figure 4c).

**TABLE 3** Comparison of trunk segment angles between leading and trailing, as well as skipping and hurdling.

		Trailing/stride		Leading		$p_{tr-le}$	$p_{SK-HU,tr}$	$p_{SK-HU,le}$
		Mean	Std	Mean	Std			
<i>lum</i>	$\alpha_{TD}$ (deg)	SK	-4.7	$\pm 6.4$	-8.0	$\pm 5.4$	n.s.	n.s.
		HU	-1.4	$\pm 4.5$	-9.3	$\pm 3.8$	2.3E-07	n.s.
	$\alpha_{LO}$ (deg)	SK	5.8	$\pm 6.0$	9.4	$\pm 5.3$	n.s.	n.s.
		HU	2.7	$\pm 3.8$	10.3	$\pm 3.5$	3.5E-15	n.s.
$\alpha_{rg}$ (deg)	SK	17.5	$\pm 8.9$	18.9	$\pm 8.5$	n.s.	n.s.	n.s.
		HU	16.2	$\pm 5.6$	20.3	$\pm 4.9$	3.0E-06	n.s.
	$\alpha_{st}$ (deg)	SK	-0.7	$\pm 3.2$				n.s.
		HU	-1	$\pm 4.4$				
$\beta_{TD}$ (deg)	SK	-3.2	$\pm 8.2$	0.3	$\pm 2.5$	n.s.	n.s.	n.s.
		HU	-9.9	$\pm 4.8$	-0.2	$\pm 3.7$	2.6E-10	n.s.
	$\beta_{LO}$ (deg)	SK	-0.3	$\pm 3.7$	2.6	$\pm 4.7$	n.s.	8.5E-10
		HU	7.9	$\pm 0.2$	6.4	$\pm 6.7$	1.1E-12	n.s.
$\beta_{rg}$ (deg)	SK	11.9	$\pm 5.3$	8.5	$\pm 3.6$	n.s.	1.6E-06	
		HU	20.3	$\pm 5.1$	16.0	$\pm 3.7$	1.7E-03	1.1E-06
	$\beta_{st}$ (deg)	SK	-4.8	$\pm 7.4$				n.s.
		HU	-10.3	$\pm 4.0$				
$\gamma_{TD}$ (deg)	SK	6.9	$\pm 5.2$	9.3	$\pm 6.4$	n.s.	n.s.	n.s.
		HU	5.0	$\pm 4.0$	0.3	$\pm 5.3$	1.5E-05	3.5E-06
	$\gamma_{LO}$ (deg)	SK	-5.0	$\pm 3.8$	-11.4	$\pm 2.8$	3.4E-04	n.s.
		HU	-0.8	$\pm 4.9$	-1.4	$\pm 4.5$	n.s.	1.5E-11
$\gamma_{rg}$ (deg)	SK	21.9	$\pm 6.7$	22.7	$\pm 6.6$	n.s.	3.2E-06	
		HU	13.3	$\pm 5.4$	10.0	$\pm 5.6$	2.4E-05	3.5E-11
	$\gamma_{st}$ (deg)	SK	-0.3	$\pm 3.8$				n.s.
		HU	-0.9	$\pm 2.3$				
<i>tho</i>	$\alpha_{TD}$ (deg)	SK	2.4	$\pm 2.8$	3.2	$\pm 2.1$	n.s.	3.2E-10
		HU	-3.8	$\pm 3.1$	2.6	$\pm 2.2$	7.0E-09	n.s.
	$\alpha_{LO}$ (deg)	SK	-2.1	$\pm 1.7$	-2.8	$\pm 2.7$	n.s.	1.7E-03
		HU	-0.2	$\pm 1.3$	-6.7	$\pm 3.3$	1.4E-17	1.2E-07
$\alpha_{rg}$ (deg)	SK	7.1	$\pm 4.7$	7.1	$\pm 4.0$	n.s.	n.s.	n.s.
		HU	8.1	$\pm 2.7$	10.0	$\pm 4.3$	n.s.	3.6E-02
	$\alpha_{st}$ (deg)	SK	-0.4	$\pm 4.0$				n.s.
		HU	0.2	$\pm 5.6$				
$\beta_{TD}$ (deg)	SK	2.3	$\pm 3.8$	-0.7	$\pm 2.2$	n.s.	n.s.	n.s.
		HU	4.4	$\pm 2.6$	2.7	$\pm 3.4$	5.8E-09	3.0E-03
	$\beta_{LO}$ (deg)	SK	-0.3	$\pm 2.0$	-2.8	$\pm 3.5$	n.s.	n.s.
		HU	-1.7	$\pm 2.2$	-3.3	$\pm 3.8$	1.1E-05	n.s.
$\beta_{rg}$ (deg)	SK	7.4	$\pm 3.0$	6.2	$\pm 2.3$	n.s.	n.s.	n.s.
		HU	9.0	$\pm 2.3$	9.5	$\pm 3.9$	n.s.	

(Continues)

TABLE 3 (Continued)

		Trailing/stride		Leading		$p_{tr-le}$	$p_{SK-HU,tr}$	$p_{SK-HU,le}$
		Mean	Std	Mean	Std			
$\beta_{st}$ (deg)	SK	-33.2	$\pm 11.9$					3.9E-08
	HU	-45.2	$\pm 14.4$					
$\gamma_{TD}$ (deg)	SK	2.3	$\pm 3.6$	0.4	$\pm 3.5$	n.s.	n.s.	
	HU	6.9	$\pm 6.6$	3.6	$\pm 3.6$	n.s.	n.s.	
$\gamma_{LO}$ (deg)	SK	-2.4	$\pm 1.7$	2.5	$\pm 4.0$	4.4E-03	n.s.	
	HU	-5.6	$\pm 3.4$	5.8	$\pm 4.0$	1.9E-16	n.s.	
$\gamma_{rg}$ (deg)	SK	10.1	$\pm 2.7$	7.7	$\pm 3.7$	6.7E-03	3.3E-04	
	HU	17.0	$\pm 5.2$	7.9	$\pm 4.1$	4.6E-17	n.s.	
$\gamma_{st}$ (deg)	SK	4.7	$\pm 14.6$					n.s.
	HU	0.7	$\pm 12.2$					
pel	$\alpha_{TD}$ (deg)	SK	-4.0	$\pm 3.3$	-4.7	$\pm 3.4$	n.s.	n.s.
		HU	-6.0	$\pm 5.0$	-6.4	$\pm 2.6$	n.s.	n.s.
	$\alpha_{LO}$ (deg)	SK	4.2	$\pm 3.1$	6.2	$\pm 2.7$	n.s.	n.s.
		HU	4.0	$\pm 3.0$	2.5	$\pm 3.9$	n.s.	3.8E-02
	$\alpha_{rg}$ (deg)	SK	11.3	$\pm 5.0$	11.2	$\pm 5.5$	n.s.	n.s.
		HU	14.4	$\pm 5.6$	9.6	$\pm 4.7$	7.9E-08	n.s.
	$\alpha_{st}$ (deg)	SK	-2.0	$\pm 6.3$				n.s.
		HU	-0.7	$\pm 9.0$				
	$\beta_{TD}$ (deg)	SK	-0.8	$\pm 5.9$	-1.3	$\pm 3.1$	n.s.	3.7E-03
		HU	-6.4	$\pm 1.8$	1.3	$\pm 2.1$	4.8E-14	n.s.
	$\beta_{LO}$ (deg)	SK	-1.6	$\pm 3.2$	0.8	$\pm 3.9$	n.s.	3.7E-12
		HU	5.6	$\pm 2.4$	3.4	$\pm 3.9$	1.7E-12	n.s.
	$\beta_{rg}$ (deg)	SK	8.4	$\pm 4.8$	7.4	$\pm 3.2$	n.s.	2.2E-06
		HU	12.9	$\pm 3.0$	9.4	$\pm 2.1$	2.6E-08	n.s.
	$\beta_{st}$ (deg)	SK	-37.5	$\pm 10.9$				1.1E-12
		HU	-55.3	$\pm 17.4$				
$\gamma_{TD}$ (deg)	SK	8.6	$\pm 4.1$	10.1	$\pm 4.5$	n.s.	n.s.	
		HU	10.7	$\pm 3.6$	5.5	$\pm 3.6$	8.4E-07	1.0E-03
$\gamma_{LO}$ (deg)	SK	-7.6	$\pm 3.7$	-9.5	$\pm 3.1$	n.s.	n.s.	
		HU	-6.5	$\pm 2.9$	1.9	$\pm 4.3$	3.6E-13	4.9E-15
$\gamma_{rg}$ (deg)	SK	20.7	$\pm 6.7$	20.0	$\pm 6.2$	n.s.	n.s.	
		HU	18.3	$\pm 5.6$	9.0	$\pm 5.4$	1.3E-10	1.7E-07
$\gamma_{st}$ (deg)	SK	4.3	$\pm 11.0$					n.s.
		HU	-0.4	$\pm 10.6$				

Note: lum, rotation between thorax and pelvis; tho, pel, rotation between thorax or pelvis and laboratory co-ordinates;  $\alpha$ ,  $\beta$ ,  $\gamma$ , cardan rotation angles, for lumbar:  $\alpha$ , lateral flexion,  $\beta$ , extension,  $\gamma$ , torsion; for thorax and pelvis:  $\alpha$ , yaw,  $\beta$ , pitch,  $\gamma$ , roll. TD, touch down; LO, lift off; rg, range; st, mean during stride; SK, skipping; HU, hurdling;  $p_{tr-le}$ , comparison between trailing leading leg;  $p_{SK-HU,tr,le}$ , comparison between skipping and hurdling for the trailing (row SK) and the leading leg (row HU). Comparisons based on GLM with repetitions (Supporting Information: Table S3) and univariate GLM (Supporting Information: Table S6) Bonferroni  $f = 336$ ; n.s.,  $p > 0.05$ .

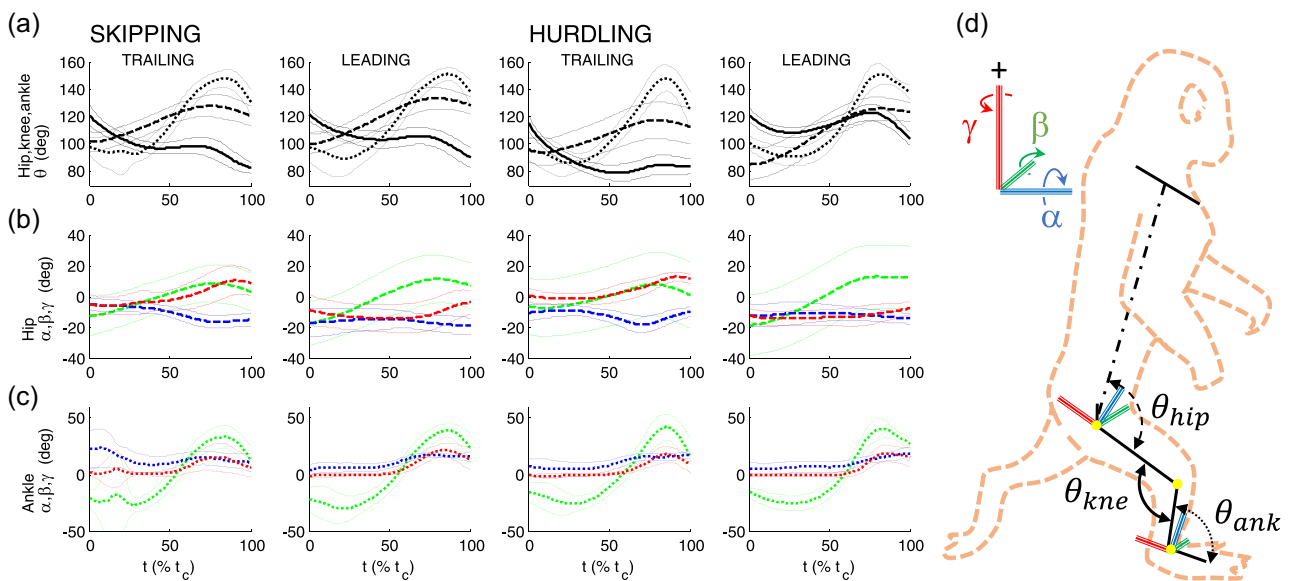


**FIGURE 2** Time course of leg angles during skipping and hurdling for the trailing and the leading leg. (a-c) Angles. (a) Enclosed angles,  $\theta$ , of the hip (dashed), knee (solid), and ankle (dotted). (b) Hip: rotation of thigh with respect to the pelvis. (c) Ankle: rotation of the foot with respect to the thigh. Rotation angles: blue, adduction  $\alpha$ ; green, extension,  $\beta$ ; red, medial rotation-means,  $\gamma$ . Bold lines are the means, thin lines are s.d. Subtracted means in  $\beta$ :  $\bar{\beta}_{\text{hip},\text{skip},\text{trail}} = -71.8\text{deg}$ ;  $\bar{\beta}_{\text{hip},\text{skip},\text{lead}} = -64.8\text{deg}$ ;  $\bar{\beta}_{\text{hip},\text{hurd},\text{trail}} = -91.1\text{deg}$ ;  $\bar{\beta}_{\text{hip},\text{hurd},\text{lead}} = -87.6\text{deg}$ ;  $\bar{\beta}_{\text{ank},\text{skip},\text{trail}} = -59.8\text{deg}$ ;  $\bar{\beta}_{\text{ank},\text{skip},\text{lead}} = -60.6\text{deg}$ ;  $\bar{\beta}_{\text{ank},\text{hurd},\text{trail}} = -67.9\text{deg}$ ;  $\bar{\beta}_{\text{ank},\text{hurd},\text{lead}} = -63.7\text{deg}$ . ISB-definitions (Wu et al., 2002):  $\text{ankleflexion}_{\text{ISB}} = \theta_{\text{ankle}} - 90\text{deg} = \beta_{\text{ankle}} + 90\text{deg}$ ;  $\text{flexion}_{\text{ISB}} \geq 0$ : *plantarflexion*;  $\text{flexion}_{\text{ISB}} < 0$ : *dorsiflexion*. Mean contact times:  $\bar{t}_{\text{c},\text{skip},\text{trail}} = (0.225 \pm 0.036\text{SD})\text{s}$ ;  $\bar{t}_{\text{c},\text{skip},\text{lead}} = (0.214 \pm 0.039\text{SD})\text{s}$ ;  $\bar{t}_{\text{c},\text{hurd},\text{trail}} = (0.240 \pm 0.033\text{SD})\text{s}$ ;  $\bar{t}_{\text{c},\text{hurd},\text{lead}} = (0.210 \pm 0.016\text{SD})\text{s}$ . d) Rotations (comp. Blickhan et al., 2021).

### 3.3 | Rotations within the trunk

Hurdling was accompanied by asymmetric trunk movements. With respect to skipping, the trunk torsion and pelvic roll were reduced. There was an individual postural bias.

**Skipping:** The trunk extended laterally ( $\alpha_{\text{lum}}$ ) at the side of the supporting leg (Figure 5a). This was largely caused by a lateral lean (yaw) of the pelvis ( $\alpha_{\text{pel}}$ ; Figure 5c) and a counter-movement of the thorax ( $\alpha_{\text{tho}}$ ; Figure 5b). The increase in dorsal flexion during the stride ( $\beta_{\text{lum}}$ ; Figure 5a) was related to a postural adjustment of the thorax while crossing the track ( $\beta_{\text{tho}}$ ; Figure 5b). Torsion ( $\gamma_{\text{lum}}$ ) of the trunk (Figure 5a) induced a considerable pelvic roll ( $\gamma_{\text{pel}}$ ; Figure 5c). In the macaque Po, the thoracic ( $\gamma_{\text{tho}}$ ) and pelvic ( $\gamma_{\text{pel}}$ ) roll were biased to the left (Figure 6f,i). Asymmetry is expressed in the thoracic roll ( $\gamma_{\text{tho-LO}}$ ) and the resulting torsion ( $\gamma_{\text{lum-LO}}$ ) at lift off (Table 3).

**Hurdling:** Trunk motion was modified for hurdling. The motion was not symmetric with respect to the contacts with the trailing and leading legs. This is expressed in thoracic values at touch down and lift off, that is, lateral lean ( $\alpha_{\text{tho-TD}}$ ,  $\alpha_{\text{tho-LO}}$ ), tilt ( $\beta_{\text{tho-TD}}$ ), roll ( $\gamma_{\text{tho-TD}}$ ), as well as in the pelvis ( $\beta_{\text{pel-TD}}$ ,  $\gamma_{\text{pel-TD}}$ ,  $\gamma_{\text{pel-LO}}$ ; Table 3). Lateral lean of the thorax started early in the trailing phase and was more in synchrony with the pelvic motion (Figure 5b,c). In contrast, in the leading phase, there was a countermovement between thorax and pelvis resulting in a strong lateral extension at the side of the leading leg ( $\alpha_{\text{lum-TD,LO}}$ ,  $\alpha_{\text{lum-rg}}$ ; Table 3). Forward tilt (pitch) of the pelvis ( $\beta_{\text{pel}}$ ) steadily increased until the beginning of the aerial phase. There was a strong dorsal extension ( $\beta_{\text{lum}}$ ; Figure 5a) from the early stance of the trailing

leg to the late stance of the leading leg ( $\beta_{\text{lum-TD,rg}}$ ; Table 3). Flexion was enhanced during the leading phase. The posture during hurdling is more lumbar extended as compared to skipping ( $\beta_{\text{lum}}$ ; Figure 6b, Table 3) and movement range was in most cases increased (Figure 5; Table 3). During the trailing phase, pelvic roll ( $\gamma_{\text{pel}}$ ) supported retraction (Figure 5c). Roll was then prolonged to almost the end of the support of the leading leg. A strong countermovement occurred in the aerial phase (Figure 5c). This was also the case for pelvic roll in the leading leg ( $\gamma_{\text{pel}}$ ; Figure 5i). Thoracic roll,  $\gamma_{\text{tho}}$ , was increased in the trailing phase. The thorax largely followed pelvic movement with a delay of about 10% T. Large torsions were observed during the aerial phase. Trunk movements largely differed between individuals (Figure 6, Supporting Information: Figure S3). The individual differences were related to differences in the duration of the aerial phase and the duration of the double support phase (Supporting Information: Figure S3C).

## 4 | DISCUSSION

### 4.1 | Skipping

Differences in global leg kinematics (Blickhan et al., 2023) suggested differential kinematics and dynamics in the leg joints. This assumption holds true especially for the hip joint. Hip extension was larger, and reached a higher speed in the leading as compared to the trailing leg ( $\beta$ ,  $\theta_{\text{hip-rg}}$ ;  $\beta$ ,  $\theta_{\text{hip-omega max}}$ ; Table 1). The leading leg was also more

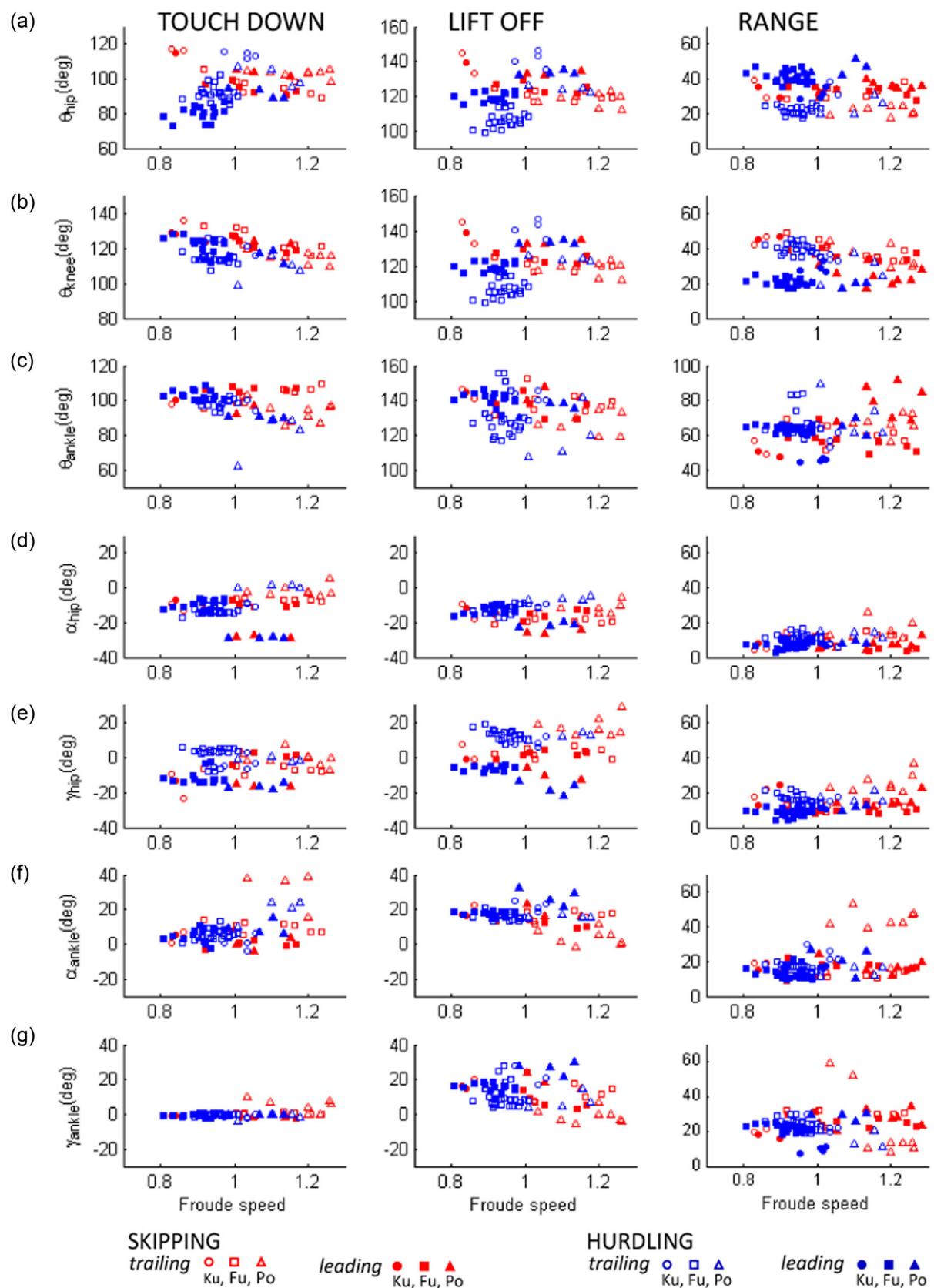


**FIGURE 3** Leg angles at touch down, and lift off, and their range during the contact in skipping and hurdling in dependence on Froude speed. Red: skipping; blue: hurdling; open: trailing leg; filled: leading leg. (a–c) Enclosed angles: (a) between thigh and HAT,  $\theta_{\text{hip}}$ ; (b) shank and thigh,  $\theta_{\text{knee}}$ ; (c) foot and thigh,  $\theta_{\text{ankle}}$ . (d–g) Rotation angles: (d) hip adduction,  $\alpha_{\text{hip}}$ ; (e) hip medial rotation,  $\gamma_{\text{hip}}$ ; (f) ankle adduction,  $\alpha_{\text{ankle}}$ ; (g) ankle medial rotation,  $\gamma_{\text{ankle}}$ . Red: skipping; blue: hurdling; open: trailing leg; filled: leading leg. Circle: Ku; square: Fu; triangle: Po.

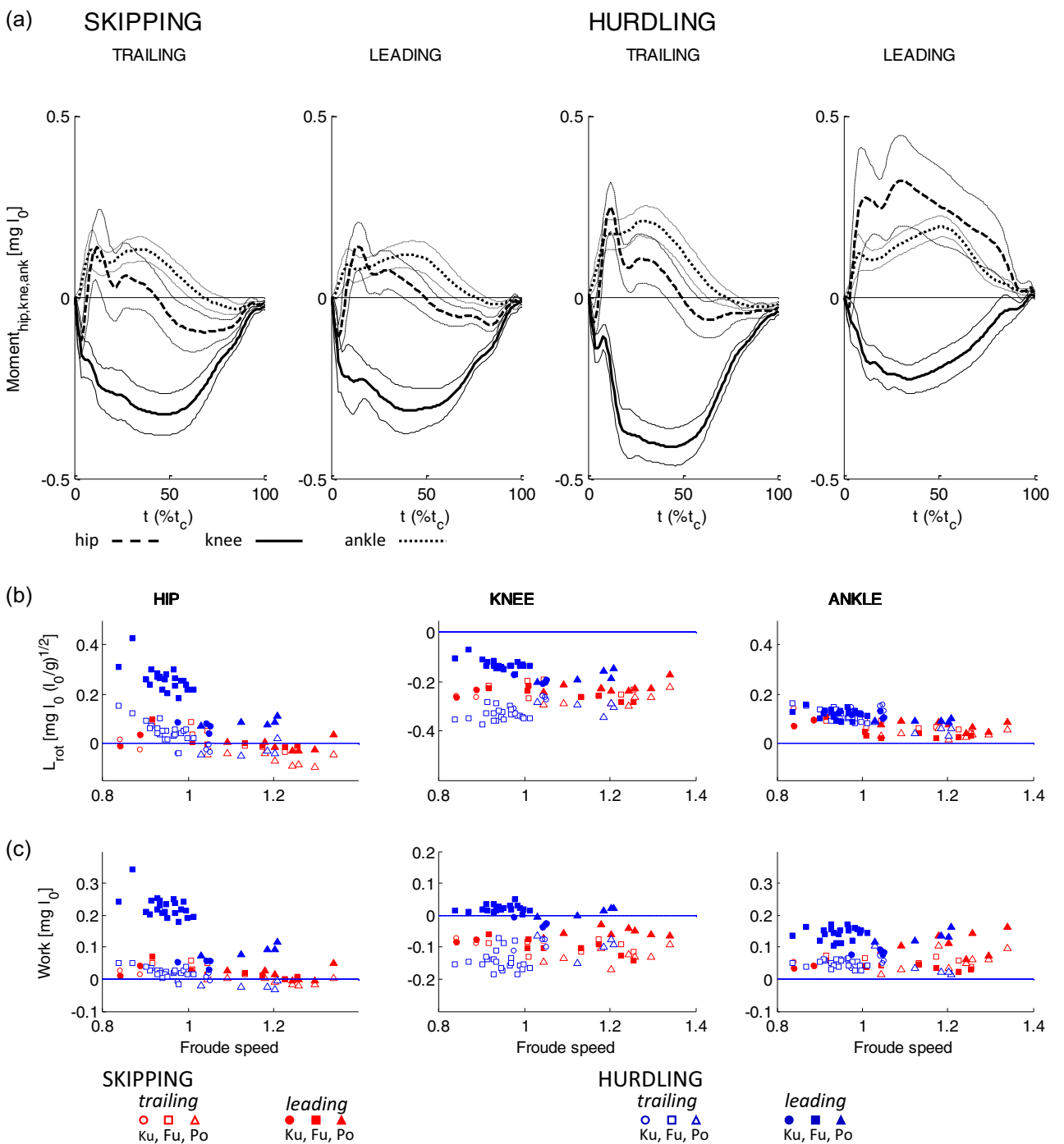


**FIGURE 4** Moments (a), rotational impulses (b), and work (c) at hip, knee, and ankle for skipping, hurdling the trailing and the leading leg, respectively. (a) Time course of joint moments 2D, from proximal to distal. Hip (dashed), knee (solid), and ankle (dotted). Bold lines are the means, thin lines are s.d. The counterclockwise momentum in the ankle is <0. (b) Rotational impulse,  $L_{rot}$ , at the hip, knee, and ankle in dependence of the Froude speed. (c) Joint work. Red: skipping; blue: hurdling; open: trailing leg; filled: leading leg. Circle: Ku; square: Fu; triangle: Po.

retracted at lift off,  $\beta, \theta_{hip-LO}$ . In contrast, the range of knee movement,  $\theta_{kne-rg}$ , was diminished and there was no difference in the range of ankle movement in the mainplane ( $\beta, \theta$ ). In both steps, leg movement was dominated by hip extension and hip flexion; the stronger hip extension in the leading leg seemed to be compensated by the reduced knee flexion. The lift of the CoM (Blickhan et al., 2023) of the leg correlated with hip movement (extension supported by

eversion). Hip abduction and lateral rotation,  $\alpha_{hip-TD}, \gamma_{hip-rg,LO}$ , supported the increased hip extension in the leading leg. The kinematics of the ankle joint had only a minor influence. Only the range of foot adduction differed strongly ( $\alpha_{ank-rg}$ ; Table 1). The macaques had problems with the placement of the foot after the leap. The rebound behavior especially of the trailing leg (Blickhan et al., 2023) was hardly reflected in the rebound of any joint. The

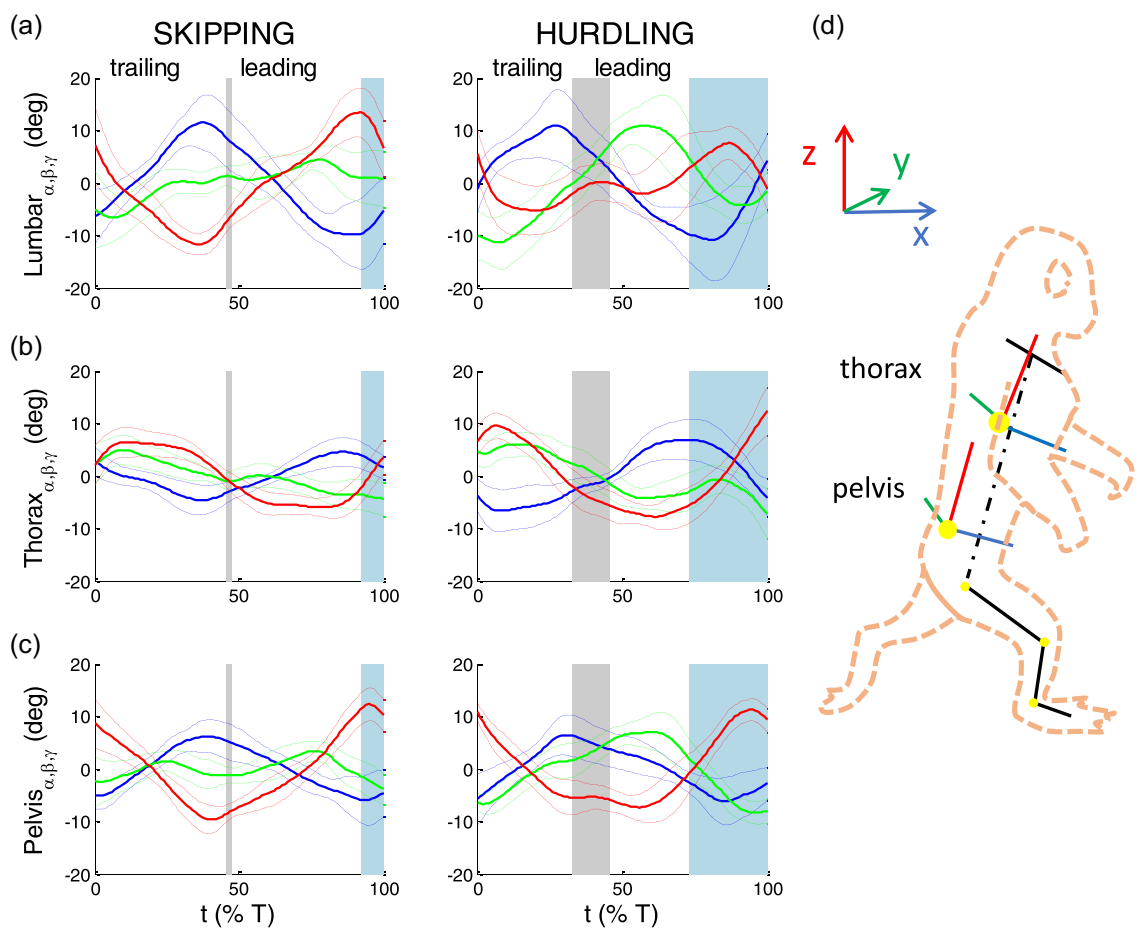


**FIGURE 5** Time course of rotations of mean angles within the trunk during skipping and hurdling. (a) Rotation of the pelvis with respect to the thorax. (b) Rotation of the thorax with respect to laboratory coordinates. (c) Rotation of the pelvis with respect to laboratory coordinates. Rotation angles: (a) blue, lateral extension  $\alpha$ ; green, extension  $\beta$ ; red, torsion  $\gamma$ ; (b, c) blue, yaw (lateral lean)  $\alpha$ ; green, pitch (forward tilt)  $\beta$ ; red roll (axial rotation)  $\gamma$ . Bold lines: means – bias subtracted; thin lines: SD. The stride (mean period T) starts with the touch down of the right trailing leg ( $t = 0\% T$ ). The dark gray strip below 50% T marks the mean double support, that is, the mean touch down of the left leading leg and the mean lift off of the right trailing leg. The light gray field at the end of the stride marks the mean aerial time starting with the lift off of the leading leg and ending with the touch down of the trailing leg. For this graph: skipping  $n = 13$ , four trials starting with the trailing leg, ignored in this graph, hurdling  $n = 32$ .  $\beta_{lumbar}$  decreasing: flexion;  $\beta_{lumbar}$  increasing: extension;  $\beta_{lumbar} = 0$  deg: thorax and pelvis aligned;  $\beta_{lumbar} < 0$  deg: thorax bent anteriorly with respect to the pelvis;  $\beta_{pelvis,thorax} = 0$  deg alignment;  $\beta_{pelvis,thorax} > 0$  deg anterior pitch of the segment. Gray shading: mean double support phase; blue shading: mean aerial phase. (d) Coordinate systems (comp. Figure 1 and Blickhan et al., 2021).

rebound at the knee was small in both legs. It was slightly higher in the ankle, but not with respect to the rebound gap. In general, the rebound of the effective leg was organized by bending of the knee and subsequent extension of the ankle joint (Figure 2).

The range of joint moments showed only slight differences in the ankle joint between the leading and trailing leg ( $M_{ank,min}$ ) and the transferred rotational impulses did not differ (Table 2). The similarity of the generated leg impulses (Blickhan et al., 2023) was confounded at the joint level. The knee must generate the highest momenta. In human bipedal locomotion, this is avoided by an extended knee. In the macaques, the high momenta at the knee were accompanied by a decrease in the enclosed knee angle. Correspondingly, there was consistent work on the knee extensors with higher values in the trailing leg (Table 2). Damping and energy absorption occurred at the knee.

The rotations of the trunk segments were largely symmetric during the stride in skipping. The different movements within the hip joint were supported by an insignificant enhancement of pelvic yaw at lift off,  $\alpha_{pel-Lo}$ , which in turn was expressed in lumbar lateral flexion at touch down and extension at lift off, ( $\alpha_{lum-TD,Lo}$ ). The preparation to leaping was accompanied by enhanced lumbar torsion,  $\gamma_{lum-Lo}$ , as well as roll of the thorax,  $\gamma_{tho-rg,Lo}$ , at lift off (Table 3). The lumbar extension,  $\beta_{lum-Lo}$ , and reduced thoracic tilt,  $\beta_{tho-Lo}$ , also noticeable in the erection,  $\beta_{tr-Lo}$ , of the trunk, was only minor.

The minor deviations from symmetric gaits, as expressed in a short double support and a short flight phase, were not accompanied by major changes in trunk kinematics. The slight reduction in hip extension in the leading step did not enforce major pelvic adjustments. However, coping with the reduced contact time in this step,

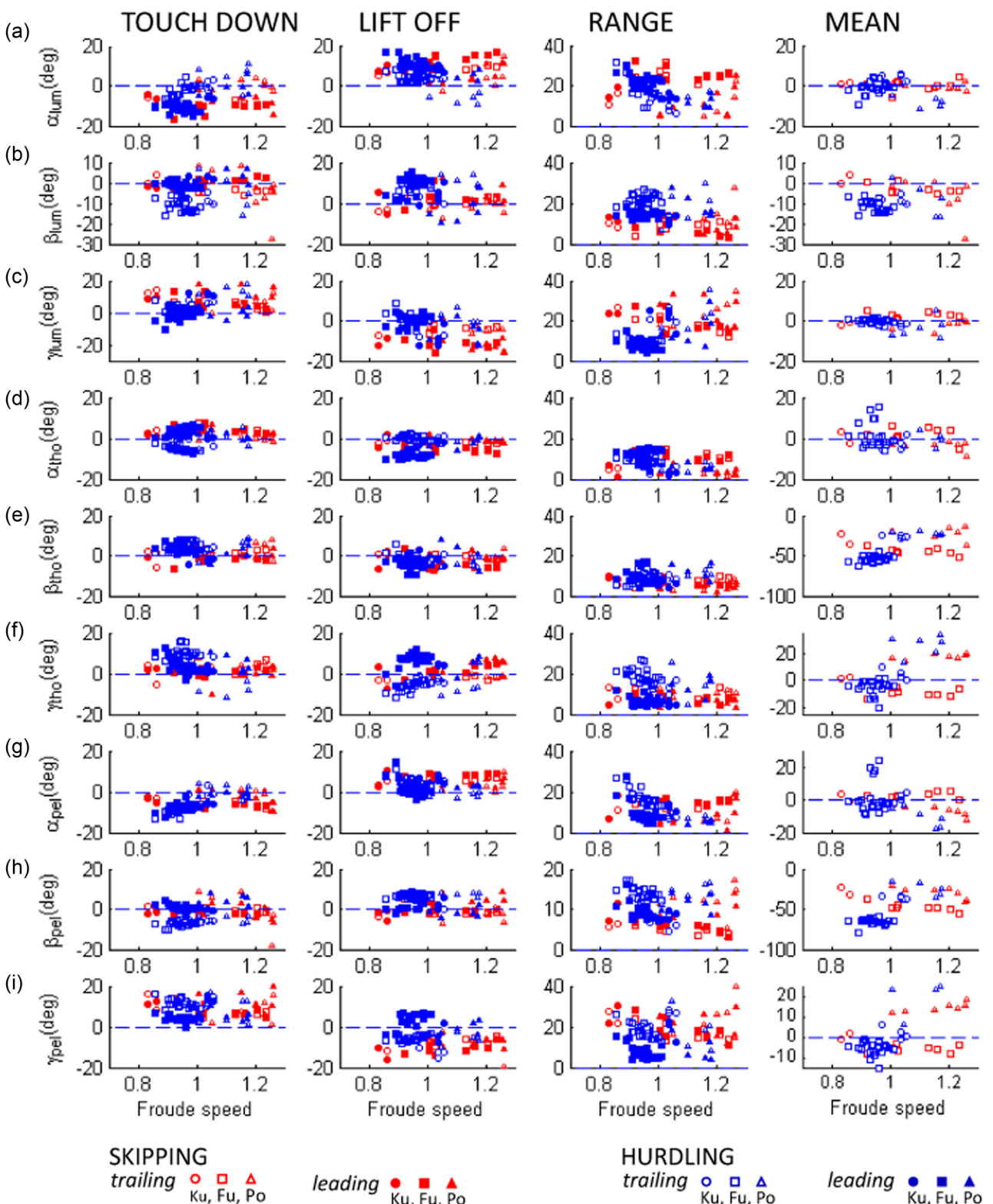


**FIGURE 6** Trunk angles at touch down, and liftoff, their step range, and the subtracted stride means during skipping and hurdling in dependence on Froude speed. Red: skipping; blue: hurdling; open: trailing leg; filled: leading leg. (a–c) Rotation between pelvis and thorax: (a) lateral flexion,  $\alpha_{lum}$ ; (b) extension,  $\beta_{lum}$ ; (c) foot and thigh,  $\gamma_{lum}$ . (d–i) Rotation of thorax (d–f) and the pelvis (g–i) with respect to laboratory coordinates: (d, g) yaw (lateral lean),  $\alpha_{tho,pel}$ ; (e, h) pitch (forward tilt),  $\beta_{tho,pel}$ ; (f, i) roll (axial rotation),  $\gamma_{tho,pel}$ .  $\beta_{lum}$  decreasing: right flexion;  $\beta_{lum}$  increasing: right extension;  $\beta_{lum} = 0$  deg: thorax and pelvis aligned;  $\beta_{lum} < 0$  deg: thorax bent anteriorly with respect to the pelvis;  $\beta_{pel,tho} = 0$  deg alignment;  $\beta_{pel,tho} > 0$  deg anterior pitch of the segment. Red: skipping; blue: hurdling; open: trailing leg; filled: leading leg. Circle: Ku; square: Fu; triangle: Po.

this was accompanied by a reduction of the rebound gap at the knee and a slightly enhanced leg stiffness (Blickhan et al., 2023). Despite quasi-elastic operation of the effective leg, the operation of the leg joints prevented a major use of elastic storage or a stretch-shortening cycle. However, the combined knee flexion in the early support phase and the extension of the ankle in the late stance may follow the minimization of leg work (Rode et al., 2016), as larger rotations are shifted to a joint with lower torque.

## 4.2 | The legs during hurdling and differences to skipping

In terms of global properties (Blickhan et al., 2023), hurdling accentuated the differences between the trailing and leading steps.

During hurdling, there was a vast difference between the legs in the range of hip extension ( $\theta, \beta_{\text{hip-rg}}$ ; Table 1). The extension of the hip of the leading leg was even higher than during skipping (Table 3). As the more flexed hip at touch down indicates, this was accompanied by the more pitched posture during hurdling (Blickhan et al., 2023). The extension at lift off was not enhanced indicating anatomical limitations. The difference of the hip extension does reflect the changes of the angles of the effective global leg (Blickhan et al., 2023), and was accompanied by the different operations of the knee ( $\theta, \beta_{\text{kne}}$ ; Table 1). The latter had a reduced operation range in the leading leg as compared to the trailing leg. The seemingly adverse strategy helped to produce considerable resilience ( $\theta_{\text{kne-nreb,ngap}}$ ) in the knee of the leading leg (Table 1). The knee extensors may take advantage of the stretch-shortening cycle, facilitating the generation of sufficient force for the leap (Bobbert et al., 1996; Cavagna et al., 1986; Tomalka et al., 2020). This quasi-elastic operation of the knee came at the cost of strong hip extension. The stronger retraction of the hip combined with the rebound in the knee enforced a stronger amortization in the ankle and a faster extension. During skipping, the differences in extension were supported and accentuated by minor differences in hip abduction and large differences in lateral rotation ( $\alpha_{\text{hip-rg,TD,LO}}, \gamma_{\text{hip-rg,TD,LO}}$ ; Table 1). Three-dimensional hip rotations played a substantial role. In the trailing leg lateral-medial rotation was close to zero, but lateral rotations were observed in the leading leg (Table 1).

The macaques generated higher joint moments,  $M$ , during hurdling than during skipping. During hurdling, differences between the leading and trailing legs were more pronounced (Figure 4; Table 2). Corresponding to the leg's rotational impulse and tangential work, the rotational work at the hip was high especially for Fu. This individual used to locomote with a strongly pitched trunk. The pitched posture seemed to foster the generation of torques at the hip joint. The rotational impulses,  $L_{\text{rot}}$ , and the rotational work,  $W_{\text{rot}}$ , at the knee strongly differed between the trailing and leading leg (Table 2). In the knee of the trailing leg, high counterclockwise rotational impulses were generated and they were reduced in the leading leg. In combination with the bending knee, the rotational impulses in the trailing leg resulted in strong absorption of energy (Figure 4; Table 2).

After landing from the flight, the knee is responsible for damping. However, in the leading leg, the combination with the rebound behavior resulted in slight extensional work done at the knee supporting the action of hip and ankle. The increased moments at the hip and the ankle seemed to enforce the eccentric loading of the knee joint. Eccentric loading in general facilitates force generation by muscles.

During hurdling, the macaques have a more pitched posture as signaled by the mean pitch of the pelvis and thorax ( $\beta_{\text{pel,tho-st}}$ ; Table 3). In addition, the mean roll of the thorax is reduced ( $\gamma_{\text{tho-st}}$ ). The trunk as a motor of leg movement (Fischer & Witte, 2007; Gracovetsky, 1985) showed strong internal asymmetries between the trailing and leading steps. This was reflected by increased pelvic yaw,  $\alpha_{\text{pel-rg}}$ , its reduced roll,  $\gamma_{\text{pel-rg,TD,LO}}$ , and its reduced pitch,  $\beta_{\text{pel-rg,LO}}$ , in the leading as compared to the trailing leg. The pelvis seemed to be stiffened. The differences at lift off indicated that roll supported leg extension in the leading leg,  $\gamma_{\text{pel-LO}}$ , but pitch,  $\beta_{\text{pel-LO}}$ , was reduced. As a consequence of the enhanced double support, the tracings lost symmetry between the trailing and leading phases (Figure 5). This was still visible in the thoracic movement ( $\gamma_{\text{tho-rg}}, \alpha, \beta_{\text{tho-TD}}, \alpha, \beta, \gamma_{\text{tho-LO}}$ ) and was accompanied by differences in lumbar lateral-flexion, flexion, and torsion ( $\alpha, \beta, \gamma_{\text{lum-rg}}, \alpha, \beta, \gamma_{\text{lum-TD}}, \alpha, \beta_{\text{lum-LO}}$ ; Table 3). Lumbar flexion lost almost completely its double periodicity typical for walking and running, where both legs operated in symmetry. This points toward a modified role of lumbar flexors and extensors. As compared to skipping, the amplitude of pelvic movement was amplified only with respect to pitch. This was accompanied by increased lumbar extension. The role of the thorax increased. Nevertheless, the range of lumbar torsion decreased pointing toward stiffening of the trunk.

Both the kinematic and kinetic properties of the legs and their joints, as well as the role of the trunk strongly supported the differential function of the trailing and leading leg. Two subjects had a preferred side (trailing leg for each individual: left|right, Ku:6|0; Fu: 11|19; Po: 0|14). The macaque Po skipped with a rotated posture as indicated by the left bias with respect to the thoracic and pelvic roll ( $\gamma_{\text{tho,pel}}$ ; Figure 6f,i). While landing from the aerial phase, subject (Po) showed skipping adjustment instabilities in the right ankle joint resulting in fast and strong changes in ankle angles ( $\alpha, \beta, \gamma_{\text{ank}}$ ; Supporting Information: Figure S1). Inspection of the video films taken revealed that in these trials, Po touched down with an inverted foot and fisted toes. This was not observed while skipping across the hurdles. As compared to the leading leg, the moments at the ankle joint were, with exceptions during early stance, during hurdling reduced in the trailing leg (Supporting Information: Figure S2). A slightly reduced impact peak indicates a more compliant touch down (Blickhan et al., 2023), which was also observed in the leading leg. However, the peak vertical forces at around midstance were elevated compared to the other subjects for both legs. Distal deviations have only minor influence on the operation of proximal joints and global dynamics. Po also pulled inside with both hind legs during skipping (Blickhan et al., 2023). As the subject enjoyed the experimental sessions and skipped with full dynamics, the differences point

toward an instable habit during bipedal locomotion. The subjects Po and Fu were both less experienced in bipedal locomotion than Ku. Inside pulling and a more supinated foot posture at touch down could indicate quadrupedal locomotion (Hirasaki et al., 2010). Individual differences in deviations in joint and leg anatomy, as well as adaptations to grasping (Gebo, 1985) cannot be excluded.

### 4.3 | Skipping in humans, macaques, and sifakas

Hip and knee of human bipedal gallopers were much more extended but the ankle only slightly more extended than those of the macaques (from Fiers et al., 2013), values at TD | LO| range during contact:  $\theta_{\text{hip,lead}} = 120 | 169 | 49\text{deg}$ ;  $\theta_{\text{kne,lead}} = 159 | 157 | 22\text{deg}$ ;  $\theta_{\text{ank,lead}} = 115 | 142 | 36\text{deg}$ ; from Whitall & Caldwell, 1992:  $\theta_{\text{hip,trail}} = 161 | 187 | 30\text{deg}$ ;  $\theta_{\text{kne,trail}} = 158 | 143 | 20\text{deg}$ ;  $\theta_{\text{ank,trail}} = 115 | 132 | 41\text{deg}$ ;  $\theta_{\text{hip,lead}} = 133 | 173 | 40\text{deg}$ ;  $\theta_{\text{kne,lead}} = 106 | 136 | 21\text{deg}$ ;  $\theta_{\text{ank,lead}} = 106 | 136 | 32\text{deg}$ ). The range of operation is rather similar in the hip of the trailing leg and the knee of the leading leg during hurdling. All other values appear to be higher in the macaque. The higher leg compliance of the macaque was expressed in an enhanced movement range of the leg joints. The observed rebound during human unilateral skipping underlined quasi-elastic operation of the trailing ankle as well as of the leading knee joint ( $\theta_{\text{kne,trail}} | \theta_{\text{ank,trail}} | \theta_{\text{kne,lead}} | \theta_{\text{ank,lead}}$ , relative rebound, nreb: after Fiers et al., 2013: 0.51 | 0.85 | 0.89 | 0.25; after Whitall & Caldwell, 1992: 0.60 | 0.58 | 0.66 | 0.30; and relative rebound gap, ngap: after Fiers et al., 2013: -0.64 | 0.15 | -0.11 | 0.75, after Whitall & Caldwell, 1992: -0.40 | 0.42 | -0.34 | 0.70). In the macaque, only the knee of the leading leg during hurdling approached human values (Table 1). In contrast to human bipedal gallopers, the macaques were not able to take advantage of quasi-elastic rebounds. Wunderlich and Schaum (2007) studied the kinematics of a lemur during unilateral skipping approaching hopping with a substantial contact time overlap of 73%  $t_c$ . The indrid displayed highly quasi-elastic movement patterns in the leg joints (after Wunderlich & Schaum, 2007: TD | LO| range during contact:  $\theta_{\text{hip}} = 91 | 167 | 90\text{deg}$ ;  $\theta_{\text{kne}} = 121 | 123 | 55\text{deg}$ ;  $\theta_{\text{ank}} = 174 | 159 | 38\text{deg}$ ; nreb:  $\theta_{\text{kne}} = 0.977$ ;  $\theta_{\text{ank}} = 0.601$ ; ngap:  $\theta_{\text{kne}} = 0.024$ ;  $\theta_{\text{ank}} = -0.399$ ). The hopping style demanded a high range of hip movement (speed not given,  $Fr \cong 1$ ). The hip of the trailing leg was strongly abducted resulting in a sideward positioning and an almost vertical position of the effective leg in the sagittal plane. In the macaque Po an enhanced abduction was observed at touch down of the leading leg. The range of knee movement in the sifaka was higher than in humans and macaques and the flexed knees even exceeded human rebound values. Flexed knees do not prevent rebound. The ankle approaches human elastic rebound too. From vertical displacement (Wunderlich & Schaum, 2007), a peak vertical leg force,  $F_z \cong 1.8[\text{mg}]$ , and a leg stiffness,  $k \cong 4[\text{mg}/l_0]$ , can be estimated. The white sifaka skipped with legs even more compliant than those observed in the macaque ( $k \cong 10[\text{mg}/l_0]$ ; Blickhan et al., 2023). Similarly, in the macaque, hurdling was enabled by increased double support, slightly enhanced leg compliance, and increased aerial

phases. By parallel operation of the legs, the stiffnesses sum up, and sufficiently short contact times were allowed by more compliant legs. This also enhanced the quasi-elastic rebound in the knee. On the other hand, the more running-like movement pattern with less double support and short aerial phases during skipping suppressed quasi-elastic rebound in the joints, but not at the level of the effective leg (Blickhan et al., 2023).

In the human subjects, the moments at the ankle of the leading leg were reduced as compared to the trailing leg and the knee moments did not differ. However, as in the hurdling macaque, the hip moments in the leading leg were enhanced (Fiers et al., 2013, Figures 1 and 5). During bilateral skipping (McDonnell et al., 2017), human subjects generated in the trailing step high rotational impulses (at  $Fr = 0.86$ ; our sign convention) in the hip and the knee ( $L_{\text{hip,trail}} | L_{\text{kne,trail}} | L_{\text{ank,trail}} = 0.135 | -0.109 | 0.086[\text{mg}l_0 \sqrt{l_0/g}]$ ) and in the leading step high rotational impulses in the ankle ( $L_{\text{hip,lead}} | L_{\text{kne,lead}} | L_{\text{ank,lead}} = 0.08 | -0.054 | 0.127[\text{mg}l_0 \sqrt{l_0/g}]$ ). The rotational impulses in the macaque's hip were lower, in the knee higher and in the ankle lower (Table 2). The extended human knee reduces joint torques. In human unilateral skipping, hip and knee of the trailing leg and the knee of the leading leg absorbed net energy during a stride whereas it produced work in the ankle of both the trailing and the leading leg as well as in its hip ( $W_{\text{hip,trail}} | W_{\text{kne,trail}} | W_{\text{ank,trail}} = -0.029 | -0.041 | 0.010[\text{mg}l_0]$ ;  $W_{\text{hip,lead}} | W_{\text{kne,lead}} | W_{\text{ank,lead}} = 0.090 | -0.023 | 0.045[\text{mg}l_0]$ ; Fiers et al., 2013). In the macaque, hip, and ankle produced work both in the trailing and leading leg and during hurdling in the knee of the leading leg. The knee absorbed energy during skipping in both legs and in the trailing leg during hurdling (Table 2). Under the assumption that the majority of mechanical work is generated during stance, the human subjects, with the exception of the leading hip, absorbed or produced in their leg joints less work during skipping than the macaque. In the hurdling macaque, especially the absorption in the trailing knee and the work in the joints of the leading leg was higher. The latter was necessary to negotiate the hurdles. The human knee operated quasi- elastically in both legs with a slight shift to absorption in the trailing leg (figures 4, 8 in Fiers et al., 2013), whereas only in the leading knee of the hurdling macaque a substantial rebound was observed (Figure 2a, Supporting Information: Figure S1a; Table 2). The flexion following the extension after about 75%  $t_c$  (Figure 2) does not substantially contribute to joint work.) In the human ankle joint the leading leg operated very similar to both leading and trailing ankle joints in the macaque. However, in the trailing leg, the human ankle showed large quasi-elastic contributions. This points toward the toe landing in the trailing leg and a rolling foot in the leading leg. In the human trailing leg, the muscles crossing the ankle and knee can take advantage of a stretch-shortening cycle. This was only possible in the knee of the hurdling macaque. An extended double support as used during hopping would probably enhance the quasi-elastic rebound.

As compared to humans, the legs of macaques operate in all running gaits including skipping more compliant (Blickhan et al., 2018, 2023) and with less rebound at the joint level (Blickhan et al., 2021). The external cost of transport calculated from the fluctuations of the mechanical energy of the CoM during unilateral

skipping was found to be of similar magnitude or higher in humans as compared to macaques (Blickhan et al., 2023). The point of operation of the musculature involved, as well as the necessary recruitment, could contribute to differences in metabolic cost. Despite unilateral skipping being the preferred fast bipedal gait for macaques in our experiments, their compliant leg and only minor rebound indicate lower efficiency in macaques compared to humans. It is worth noting that the macaques were not trained for long-distance running.

## ACKNOWLEDGMENTS

The authors express our gratitude to all the staff of the Suo Monkey Performance Association for their generous collaborations in these experiments. Thanks are due to Naoki Kitagawa, Kohta Ito, Hideki Oku, and Mizuki Tani from Keio University, Yokohama, Japan, and Martin Götze Friedrich-Schiller University, Jena, Germany, for helping us during data collection. The authors also thank Ryoji Hayakawa, ArchiveTips, Inc., Tokyo, Japan, for support and preprocessing with Qualisys. The authors would like to thank Keio University for the guest professorship appointment to R.B. strongly facilitating this line of research. Supported by a research initiation grant of the DFG to R.B. (BL 236/28-1), and Grant-in-Aid for Scientific Research (#10252610, #17H01452, #20H05462, and #22H04769) from the Japan Society of Promotion of Science and a Cooperative Research Fund of the Primate Research Institute, Kyoto University to N.O., DFG FI 410/16-1 grant as part of the NSF/CIHR/DFG/FRQ/UKRI-MRC Next Generation Networks for Neuroscience Program to E.A. Open Access funding enabled and organized by Projekt DEAL.

## DATA AVAILABILITY STATEMENT

The data that support the findings of this study are openly available in Macaque\_Skipping\_MIIla at <https://figshare.com/>, reference number <https://doi.org/10.6084/m9.figshare.24073620>.

## ORCID

Reinhard Blickhan  <http://orcid.org/0000-0001-6751-5621>

Emanuel Andrade  <http://orcid.org/0000-0002-9300-4056>

Naomichi Ogihara  <http://orcid.org/0000-0002-1697-9263>

## REFERENCES

Alexander, R. M. (2004). Bipedal animals, and their differences from humans. *Journal of Anatomy*, 204, 321–330.

Blickhan, R., Andrade, E., Hirasaki, E., & Ogihara, N. (2018). Global dynamics of bipedal macaques during grounded and aerial running. *Journal of Experimental Biology*, 221, jeb178897.

Blickhan, R., Andrade, E., Hirasaki, E., & Ogihara, N. (2021). Trunk and leg kinematics of grounded and aerial running in bipedal macaques. *The Journal of Experimental Biology*, 224, jeb225532.

Blickhan, R., Andrade, E., Hirasaki, E., & Ogihara, N. (2023). Skipping without and with hurdles in the bipedal macaque: Global mechanics. *bioRxiv*. Preprint posted online August 27, 2023. <https://doi.org/10.1101/2023.08.26.554925>

Bobbert, M. F., Gerritsen, K.G.M., Litjens, M.C.A., & Van Soest, A.J. (1996). Why is countermovement jump height greater than squat jump height? *Medicine & Science in Sports & Exercise*, 28, 1402–1412.

Cavagna, G. A., Dusman, B., & Margaria, R. (1968). Positive work done by a previously stretched muscle. *Journal of Applied Physiology*, 24, 21–32.

Fiers, P., De Clercq, D., Segers, V., & Aerts, P. (2013). Biomechanics of human bipedal gallop: Asymmetry dictates leg function. *The Journal of Experimental Biology*, 216, 1338–1349.

Fischer, M. S., & Witte, H. (2007). Legs evolved only at the end!. *Philosophical Transactions of the Royal Society A: Mathematical, Physical and Engineering Sciences*, 365, 185–198.

Gebo, D. L. (1985). The nature of the primate grasping foot. *American Journal of Biological Anthropology*, 67, 269–277.

Gracovetsky, S. (1985). An hypothesis for the role of the spine in human locomotion: A challenge to current thinking. *Journal of Biomedical Engineering*, 7, 205–216.

Hayes, G., & Alexander, R. M. (1983). The hopping gaits of crows (Corvidae) and other bipeds. *Journal of Zoology*, 200, 205–213.

Hildebrand, M. (1977). Analysis of asymmetrical gaits. *Journal of Mammalogy*, 58, 131–156.

Hirasaki, E., Higurashi, Y., & Kumakura, H. (2010). Brief communication: Dynamic plantar pressure distribution during locomotion in Japanese macaques (*Macaca fuscata*). *American Journal of Physical Anthropology*, 142, 149–156.

Kimura, T. (1992). Hindlimb dominance during primate high-speed locomotion. *Primates*, 33, 465–476.

Maus, H. M., Lipfert, S. W., Gross, M., Rummel, J., & Seyfarth, A. (2010). Upright human gait did not provide a major mechanical challenge for our ancestors. *Nature Communications*, 1, 70.

McDonnell, J., Willson, J. D., Zwetsloot, K. A., Houmard, J., & DeVita, P. (2017). Gait biomechanics of skipping are substantially different than those of running. *Journal of Biomechanics*, 64, 180–185.

Minetti, A. E. (1998). The biomechanics of skipping gaits: A third locomotion paradigm? *Proceedings of the Royal Society of London Series B: Biological Sciences*, 265, 1227–1235.

Müller, R., & Andrade, E. (2018). Skipping on uneven ground: Trailing leg adjustments simplify control and enhance robustness. *Royal Society Open Science*, 5, 172114.

Nakatsukasa, M., Hirasaki, E., & Ogihara, N. (2006). Energy expenditure of bipedal walking is higher than that of quadrupedal walking in Japanese macaques. *American Journal of Physical Anthropology*, 131, 33–37.

Nakatsukasa, M., Ogihara, N., Hamada, Y., Goto, Y., Yamada, M., Hirakawa, T., & Hirasaki, E. (2004). Energetic costs of bipedal and quadrupedal walking in Japanese macaques. *American Journal of Physical Anthropology*, 124, 248–256.

Ogihara, N., Aoi, S., Sugimoto, Y., Tsuchiya, K., & Nakatsukasa, M. (2011). Forward dynamic simulation of bipedal walking in the Japanese macaque: Investigation of causal relationships among limb kinematics, speed, and energetics of bipedal locomotion in a nonhuman primate. *American Journal of Physical Anthropology*, 145, 568–580.

Ogihara, N., Hirasaki, E., Andrade, E., & Blickhan, R. (2018). Bipedal gait versatility in the Japanese macaque (*Macaca fuscata*). *Journal of Human Evolution*, 125, 2–14.

Ogihara, N., Hirasaki, E., Kumakura, H., & Nakatsukasa, M. (2007). Ground-reaction-force profiles of bipedal walking in bipedally trained Japanese monkeys. *Journal of Human Evolution*, 53, 302–308.

Ogihara, N., Makishima, H., Aoi, S., Sugimoto, Y., Tsuchiya, K., & Nakatsukasa, M. (2009). Development of an anatomically based whole-body musculoskeletal model of the Japanese macaque (*Macaca fuscata*). *American Journal of Physical Anthropology*, 139, 323–338.

Pequera, G., Ramírez Paulino, I., & Biancardi, C. M. (2021). Common motor patterns of asymmetrical and symmetrical bipedal gaits. *PeerJ*, 9, e11970.

Prins, M. R., Bruijn, S. M., Meijer, O. G., van der Wurff, P., & van Dieën, J. H. (2019). Axial thorax-pelvis coordination during gait is not predictive of apparent trunk stiffness. *Scientific Reports*, 9, 1066.

Rode, C., Sutedja, Y., Kilbourne, B. M., Blickhan, R., & Andrada, E. (2016). Minimizing the cost of locomotion with inclined trunk predicts crouched leg kinematics of small birds at realistic levels of elastic recoil. *The Journal of Experimental Biology*, 219, 485–490.

Roncesvalles, M. N. C., Woollacott, M. H., & Jensen, J. L. (2001). Development of lower extremity kinetics for balance control in infants and young children. *Journal of Motor Behavior*, 33, 180–192.

Schmitt, D. (2003). Insights into the evolution of human bipedalism from experimental studies of humans and other primates. *Journal of Experimental Biology* 206, 1437–1448.

Snyder, M. L., & Schmitt, D. (2018). Effects of aging on the biomechanics of Coquerel's sifaka (*Propithecus coquereli*): Evidence of robustness to senescence. *Experimental Gerontology*, 111, 235–240.

Tomalka, A., Weidner, S., Hahn, D., Seiberl, W., & Siebert, T. (2020). Cross-bridges and sarcomeric non-cross-bridge structures contribute to increased work in stretch-shortening cycles. *Frontiers in Physiology*, 11, 921.

Verstappen, M., Aerts, P., & Damme, R.V. (2000). Terrestrial locomotion in the black-billed magpie: Kinematic analysis of walking, running and out-of-phase hopping. *Journal of Experimental Biology*, 203, 2159–2170.

Vielemeyer, J., Grießbach, E., & Müller, R. (2019). Ground reaction forces intersect above the center of mass even when walking down visible and camouflaged curbs. *Journal of Experimental Biology*, 222, jeb204305.

Vilensky, J. A. (1983). Gait characteristics of two macaques, with emphasis on relationships with speed. *American Journal of Physical Anthropology* 61, 255–265.

Whitall, J., & Caldwell, G. E. (1992). Coordination of symmetrical and asymmetrical human gait. *Journal of Motor Behavior*, 24, 339–353.

Wu, G., Siegler, S., Allard, P., Kirtley, C., Leardini, A., Rosenbaum, D., Whittle, M., D'Lima, D. D., Cristofolini, L., Witte, H., Schmid, O., Stokes, I., & Standardization and Terminology Committee of the International Society of Biomechanics. (2002). ISB recommendation on definitions of joint coordinate system of various joints for the reporting of human joint motion—part I: ankle, hip, and spine. *J. Biomech.* 35, 543–548.

Wunderlich, R. E., & Schaum, J. C. (2007). Kinematics of bipedalism in *Propithecus verreauxi*. *Journal of Zoology*, 272, 165–175.

## SUPPORTING INFORMATION

Additional supporting information can be found online in the Supporting Information section at the end of this article.

**How to cite this article:** Blickhan, R., Andrada, E., Hirasaki, E., & Ogihara, N. (2024). Differential leg and trunk operation during skipping without and with hurdles in bipedal Japanese macaque. *Journal of Experimental Zoology Part A: Ecological and Integrative Physiology*, 341, 525–543.

<https://doi.org/10.1002/jez.2803>